gebiology

Geobiology (2016), **14**, 317–343 DOI: 10.1111/gbi.12175

Lithostratigraphic analysis of a new stromatolite–thrombolite reef from across the rise of atmospheric oxygen in the Paleoproterozoic Turee Creek Group, Western Australia

E. BARLOW,[1,2] M. J. VAN KRANENDONK,[1,2] K. E. YAMAGUCHI,[3] M. IKEHARA[4] AND A. LEPLAND[5,6]

[1]*Australian Centre for Astrobiology, University of New South Wales, Kensington, NSW, Australia*
[2]*Australian Research Council Centre of Excellence for Core to Crust Fluid Systems, Perth, Australia*
[3]*Department of Chemistry, Toho University, Tokyo, Japan*
[4]*Centre for Advanced Marine Core Research, Kochi University, Nankoku, Japan*
[5]*Geological Survey of Norway, Trondheim, Norway*
[6]*Institute of Geology, Tallinn University of Technology, Tallinn, Estonia*

ABSTRACT

This study describes a previously undocumented dolomitic stromatolite–thrombolite reef complex deposited within the upper part (Kazput Formation) of the *c.* 2.4–2.3 Ga Turee Creek Group, Western Australia, across the rise of atmospheric oxygen. Confused by some as representing a faulted slice of the younger *c.* 1.8 Ga Duck Creek Dolomite, this study describes the setting and lithostratigraphy of the 350-m-thick complex and shows how it differs from its near neighbour. The Kazput reef complex is preserved along 15 km of continuous exposure on the east limb of a faulted, north-west-plunging syncline and consists of 5 recognisable facies associations (A–E), which form two part regressions and one transgression. The oldest facies association (A) is characterised by thinly bedded dololutite–dolarenite, with local domical stromatolites. Association B consists of interbedded columnar and stratiform stromatolites deposited under relatively shallow-water conditions. Association C comprises tightly packed columnar and club-shaped stromatolites deposited under continuously deepening conditions. Clotted (thrombolite-like) microbialite, in units up to 40 m thick, dominates Association D, whereas Association E contains bedded dololutite and dolarenite, and some thinly bedded ironstone, shale and black chert units. Carbon and oxygen isotope stratigraphy reveals a narrow range in both $\delta^{13}C_{carb}$ values, from −0.22 to 0.97‰ (VPDB: average = 0.68‰), and $\delta^{18}O$ values, from −14.8 to −10.3‰ (VPDB), within the range of elevated fluid temperatures, likely reflecting some isotopic exchange. The Kazput Formation stromatolite–thrombolite reef complex contains features of younger Paleoproterozoic carbonate reefs, yet is 300–500 Ma older than previously described Proterozoic examples worldwide. Significantly, the microbial fabrics are clearly distinct from Archean stromatolitic marine carbonate reefs by way of containing the first appearance of clotted microbialite and large columnar stromatolites with complex branching arrangements. Such structures denote a more complex morphological expression of growth than previously recorded in the geological record and may link to the rise of atmospheric oxygen.

Received 07 April 2015; accepted 26 December 2015

Corresponding author: E. Barlow. Tel.: +61466324411; fax: +61293853327; e-mail: evbarlow@gmail.com

INTRODUCTION

The rise in atmospheric oxygen, or the Great Oxidation Event (GOE: Holland, 2002), at *c.* 2.3 Ga was a tipping point in Earth's history where the oxygen produced from cyanobacterial photosynthesis caused an irreversible rise in free atmospheric oxygen, which eventually resulted in the development of more complex life (Margulis & Sagan, 1997; Farquhar *et al.*, 2000; Farquhar & Wing, 2003; Goldblatt *et al.*, 2006; Papineau, 2010).

The timing of the GOE is constrained by a change in rock types (Holland, 1994), as well as by the documented change in ratios of both the mass-dependent and mass-independent fractionation of the stable isotopes of sulphur (e.g. Farquhar *et al.*, 2000; Williford *et al.*, 2011). The disappearance of mass-independent fractionation of sulphur (MIF-S: $\Delta^{33}S$) anomalies after 2.4 Ga, and the associated substantial increase in oxygen between *c.* 2.41 and *c.* 2.32 Ga (Hannah *et al.*, 2004), was recognised by Holland (2006) as the key signature of this revolutionary and irreversible change in Earth's atmosphere (see also Van Kranendonk, 2014).

Our knowledge of life's adaptation to the GOE is limited by a paucity of well-preserved stromatolitic carbonate rocks from around the globe. In order to fill this gap, we herein detail a previously undocumented, well-preserved dolomitic stromatolite–thrombolite reef complex from the *c.* 2.4–2.3 Ga Kazput Formation of the Turee Creek Group, Western Australia. This reef complex contains the first appearance of both extensive clotted (thrombolite-like) microbialites and columnar stromatolites with complex branching forms. Compared with older Neoarchean examples, including the *c.* 2.6–2.5 Ga Campbellrand Subgroup and the *c.* 2.6 Ga Carawine Dolomite, the morphological development of the Kazput reef complex attests to a more complex expression of growth than previously recorded in the geological record. We speculate that this may relate either to microbial evolution driven by the GOE, and/or community adaptation to the GOE.

GEOLOGICAL SETTING

The predominately clastic sedimentary rock succession of the approximately 4-km-thick Paleoproterozoic Turee Creek Group in the southern part of the Hamersley Ranges in Western Australia comprises the lower Kungarra, middle Koolbye and upper Kazput Formations (Trendall, 1981; Thorne & Tyler, 1996). Conformably underlain by the Boolgeeda Iron Formation of the *c.* 2.63–2.45 Ga Hamersley Group (Trendall *et al.*, 2004), the Kungarra Formation consists of approximately 3 km of primarily fine-grained sandstone, siltstone and mudstone, with two units of glaciogenic diamictite (Martin, 1999; Williford *et al.*, 2011; Van Kranendonk & Mazumder, 2015; Van Kranendonk *et al.*, 2015). The Koolbye Formation contains mature quartz-rich sandstone deposited in a mixed coastal-terrestrial environment, with abundant ripple and cross-stratification (Mazumder *et al.*, 2015). The overlying Kazput Formation consists of mixed carbonate and siliciclastic rocks, including thick dolomitic intervals (Martin *et al.*, 2000; Martindale *et al.*, 2015). The Turee Creek Group has been subjected to low-grade (prehnite–pumpellyite–epidote) metamorphism (Smith *et al.*, 1982), and the region has been affected by four phases of deformation, including two main phases of folding, where an early phase of upright folds on east–west axes is overprinted by later generations of upright, tight folds on north-west–south-east striking axial planes (Fig. 1).

The Turee Creek Group is unconformably overlain by the Wyloo Group (Martin *et al.*, 2000), which includes a lower succession of terrestrial quartz-rich sandstone, conglomerate and siltstone known as the Beasley River Quartzite (Mazumder & Van Kranendonk, 2013), and the overlying Cheela Springs Basalt. The upper part of the Wyloo Group includes the *c.* 2.03 Wooly Dolomite, the Mt. McGrath Formation, the *c.* 1.8 Ga Duck Creek Dolomite and the *c.* 1.79 Ga June Hill Volcanics (Fig. 1; Evans *et al.*, 2003; Müller *et al.*, 2005; Wilson *et al.*, 2010).

The minimum age of the Turee Creek Group is >2209 ± 15 Ma, provided by SHRIMP U-Pb zircon dating of the Cheela Springs Basalt (Martin *et al.*, 1998). The maximum age of the Turee Creek Group is constrained by a 2449 ± 3 Ma SHRIMP U-Pb zircon date of the Woongarra Rhyolite (Barley *et al.*, 1997), which conformably underlies the Boolgeeda Iron Formation at the top of the Hamersley Group. The Meteorite Bore Member (MBM) of the Kungarra Formation contains a dolerite sill with a U-Pb baddeleyite age of 2208 ± 15 Ma (Müller *et al.*, 2005). This sill is interpreted to be coeval with the eruption of the Cheela Springs Basalt; however, precise age relationships of these units are controversial (Martin & Morris, 2010). A sample of detrital zircons from diamictite in the MBM designates a maximum age of deposition of approximately 2420 Ma (Takehara *et al.*, 2010). Sulphur isotopic data were used by Williford *et al.* (2011) and Swanner *et al.* (2013) to conclude that the MBM was deposited towards the end of the GOE.

Although all previous publications have ascribed the rocks of the study area to the Turee Creek Group (Trendall & Blockley, 1970; Martin *et al.*, 2000; Van Kranendonk, 2010), concern was raised during a recent fieldtrip that the dolomitic unit studied here may represent a sliver of the younger *c.* 1.8 Ga Duck Creek Dolomite (DCD), on account of composition, proximity and apparent stratigraphic similarities (A. Knoll, pers. comm., 2012). However, as detailed below, we provide a range of evidence to indicate that the studied ridge, the Kazput Formation of the Turee Creek Group, is in fact distinct from, and cannot be, the DCD.

METHODS

Field techniques and optical microscopy

The type and extent of stromatolitic and non-stromatolitic facies were mapped in a series of 14 detailed measured transects, spaced approximately 1 km apart along the dolo-

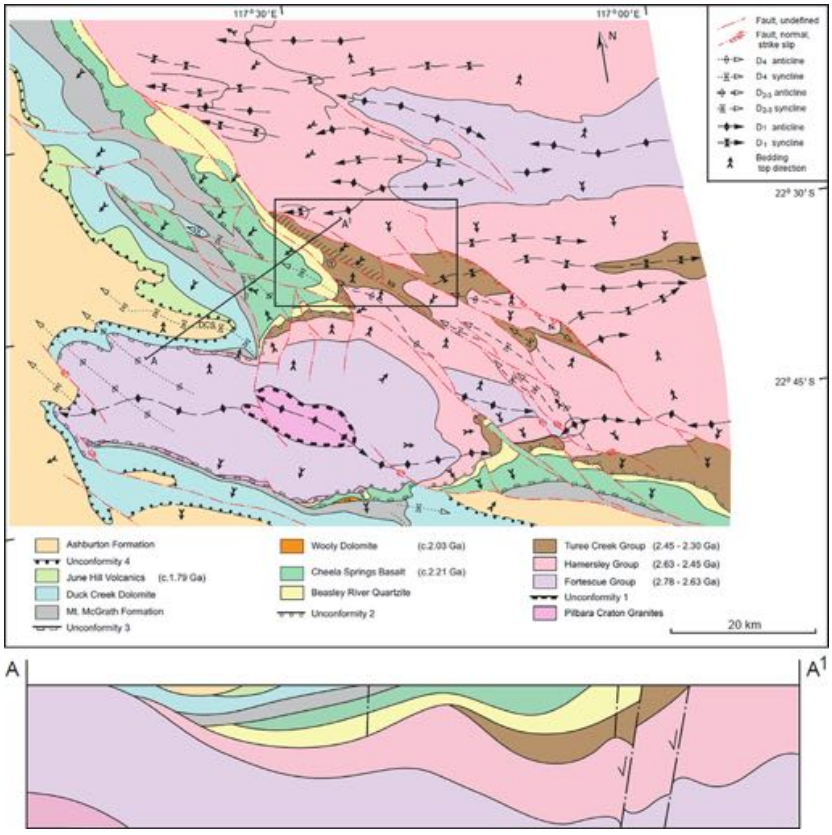

Fig. 1 Regional geological map showing the location of the Turee Creek Group within the folded rocks of the Hamersley and lower Wyloo groups. Note the simple fold geometry of the Duck Creek Dolomite and the consistent stratigraphic succession across the map area. Map collated from data presented in Blight *et al.* (1986) and Martin *et al.* (2000) and from new, detailed mapping and interpretation of aerial photographs. The black box indicates the location of Fig. 2, whilst the hashed pattern within the box shows the extent of the outcrop in this study: the Kazput reef complex. The circled number one within the black box signifies an area where rocks of the Kazput Formation are unconformably overlain by the lower Wyloo Group, and 'ks' refers to the Kazput Syncline. Line A–A^1 on the map represents the line of cross section A–A^1 shown below the map. The cross section is at an expanded scale compared to the map; however the vertical scale is equal to the horizontal scale.

mitic stromatolite–thrombolite reef complex (Barlow, 2014). Only 11 of these transects were used for final analysis due to the lack of continuous rock outcrop along Transects 6, 7 and 13. Strike and dip data were collected using a Brunton compass, and a description, sample and photograph of relevant units were documented by location. The true thickness of units was obtained by measuring the width of the unit perpendicular to strike and then calculated by trigonometry using the dip of the unit and the slope of the topography across the section. The software program PSICAT (Paleontological Stratigraphic Interval Construction and Analysis Tool) was utilised to create detailed stratigraphic columns of each transect, which were then positioned according to their GPS location along strike.

Optical microscopic analyses of petrographic thin sections was undertaken on samples collected from facies with distinct microbial textures and sedimentological features using a Leica DM2500P microscope at the University of New South Wales, Australia. A full documentation of photomicrographed samples is presented in Barlow (2014).

Raman spectroscopy

Samples of dolomitic microbialite, in which organic material (kerogen) was observed under petrographic microscope, were analysed on a Renishaw inVia Raman Microscope using a 514 nm (green) Argon ion laser with 1800 L mm^{-1} grating at the Mark Wainwright Analytical Centre of the University of New South Wales, Australia. Raman data were initially obtained with an extended scan, from ~200 to ~3200 cm^{-1}. This was followed by a static scan centred at ~1450 cm^{-1}, targeting the range between ~1000 and ~1900 cm^{-1}, allowing the acquisition of the major kerogen bands centred at ~1350 cm^{-1} (D band) and ~1600 cm^{-1} (G band). GRAMS spectroscopy software was used for data processing, specifically baseline correction to account for the spectra fluorescence in carbonate samples, and peak picking (see Supporting Information).

Carbon and oxygen isotopic analyses

Powdered bulk dolomite samples were reacted with 100% anhydrous phosphoric acid (H_3PO_4) for 800 s at 90 °C. The released CO_2 was purified and analysed for carbon and oxygen isotope compositions using an isotope ratio mass spectrometer (IsoPrime, GV Instruments, UK) installed at the Center for advanced Marine Core Research (CMCR), Kochi University, Japan. The analytical precision was better than 0.05‰ for the carbon isotope ratio and 0.06‰ for the oxygen isotope ratio of standard reference material NBS-19 [carbonate standard distributed by the International Atomic Energy Agency (IAEA)]. The results

are expressed using standard delta notation with reference to the Vienna Pee Dee Belemnite (VPDB) standard.

LITHOSTRATIGRAPHY

The dolomitic stromatolite–thrombolite reef complex studied here was first identified by Trendall & Blockley (1970) and later described by Martin *et al.* (2000) as belonging to the Kazput Formation of the Turee Creek Group. The reef complex dips on average 37° SW and faces in that direction on the eastern limb of the tight, faulted, north-west-plunging Kazput Syncline that is located to the east of the younger, and larger-scale, Duck Creek Syncline (labelled DCS; Fig. 1). A folded unit of rippled medium to coarse-grained, quartz-rich sandstone that lies stratigraphically below, to the south-east and south of the reef complex

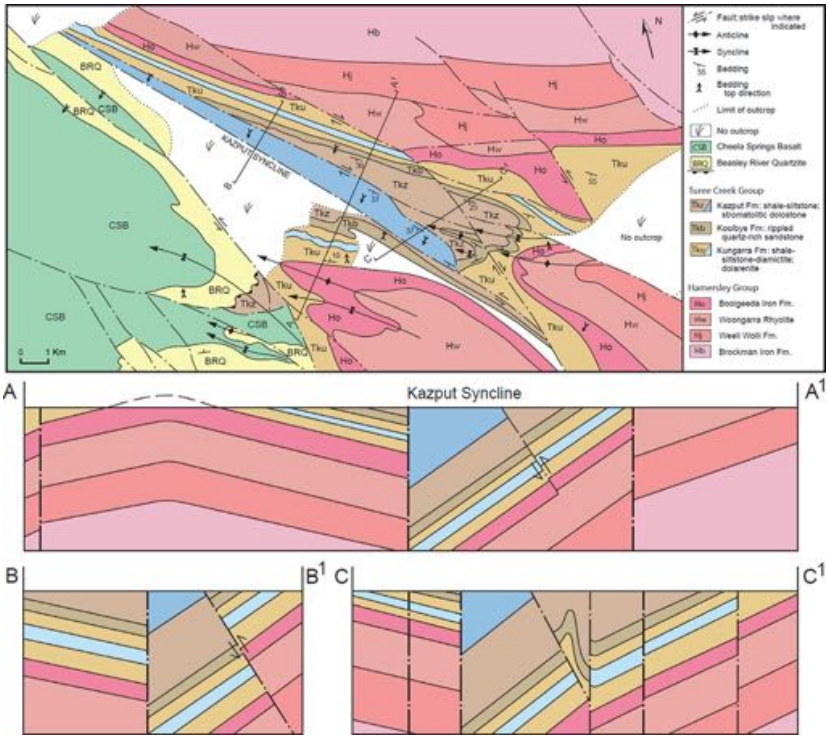

Fig. 2 Detailed geological map of the study area, showing the Kazput Formation stromatolitic dolostone in darker blue. This unit forms the eastern limb of the north-west plunging Kazput Syncline, the axial trace of which is marked by a fault (above 'Kazput Syncline' label). Lines A–A^1, B–B^1 and C–C^1 denote the location of the cross sections, which are drawn at an expanded scale compared to the map, but with the vertical scale equal to the horizontal scale.

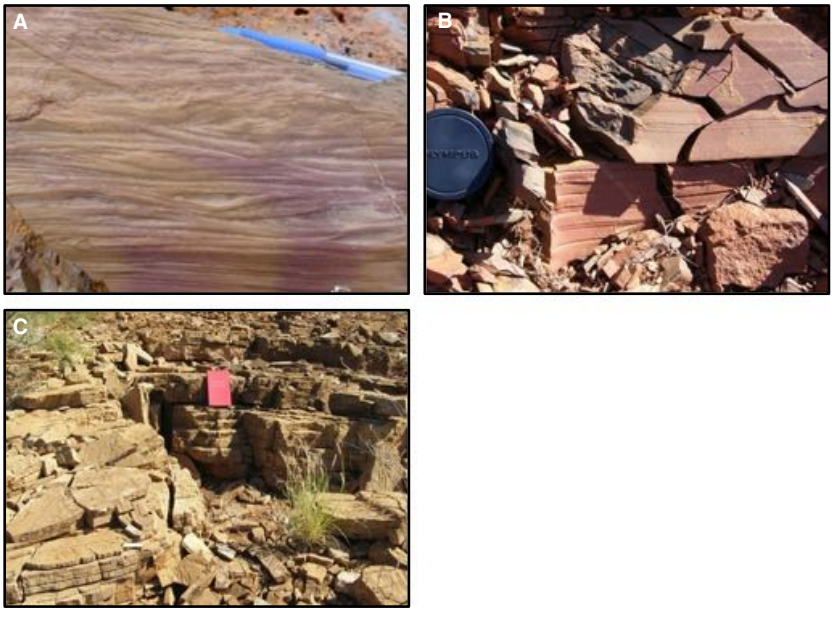

Fig. 3 Outcrop photographs of Turee Creek Group lithology from the eastern limb of the Kazput Syncline: (A) rippled quartz-rich sandstone of the Koolbye Formation. (B) Thinly bedded siltstone–mudstone of the Kungarra Formation. (C) Thinly bedded dololutite of the Kungarra Formation.

(Figs 2 and 3A), is lithologically and stratigraphically consistent with the Koolbye Formation. These rocks are underlain to the north-east by fine-grained siltstone–mudstone with units of thinly bedded dololutite (Figs 3B,C). These units also dip gently and young to the south-west and are characteristic of the Kungarra Formation (Fig. 2; Van Kranendonk *et al.*, 2015). The lowermost part of the Turee Creek Group stratigraphy on this eastern limb is excised by a north-west-south-east striking fault that separates these rocks from the older Hamersley Group (Fig. 1). Similarly, the upper contact of the reef complex is cut by the fault that lies along the axial trace of the Kazput Syncline (Fig. 2).

The western limb of the Kazput Syncline preserves a continuous, conformable section through the upper part of the Hamersley Group and lower part of the Turee Creek Group, including the conformable contact between the two (Figs 2 and 4; Williford *et al.*, 2011; Van Kranendonk *et al.*, 2015). These rocks dip gently to the north-east and face in that direction towards the faulted axis of the Kazput Syncline (Fig. 2). The lower part of the Turee Creek Group in this area comprises the diamictite of the Meteorite Bore Member of the Kungarra Formation (Williford *et al.*, 2011; Van Kranendonk *et al.*, 2015). This is conformably overlain by siltstone–mudstone and thinly bedded dololutite of the upper Kungarra Formation, which is identical to lithologies preserved on the eastern limb of the Kazput Syncline (Fig. 4). A unit of rippled, quartz-rich sandstone of the Koolbye Formation also occurs on both limbs of the syncline; near the top of the preserved succession on the western limb, and between the Kungarra and Kazput Formations on the eastern limb (Figs 2 and 4). The stratigraphic similarities on both limbs of the Kazput Syncline support correlation of these units as belonging to the Turee Creek Group, as indicated by previous authors, with the reef complex on the eastern limb of the Kazput Syncline studied here representing a higher stratigraphic level than preserved on the western limb of the syncline (Fig. 2; Trendall & Blockley, 1970; Martin *et al.*, 2000).

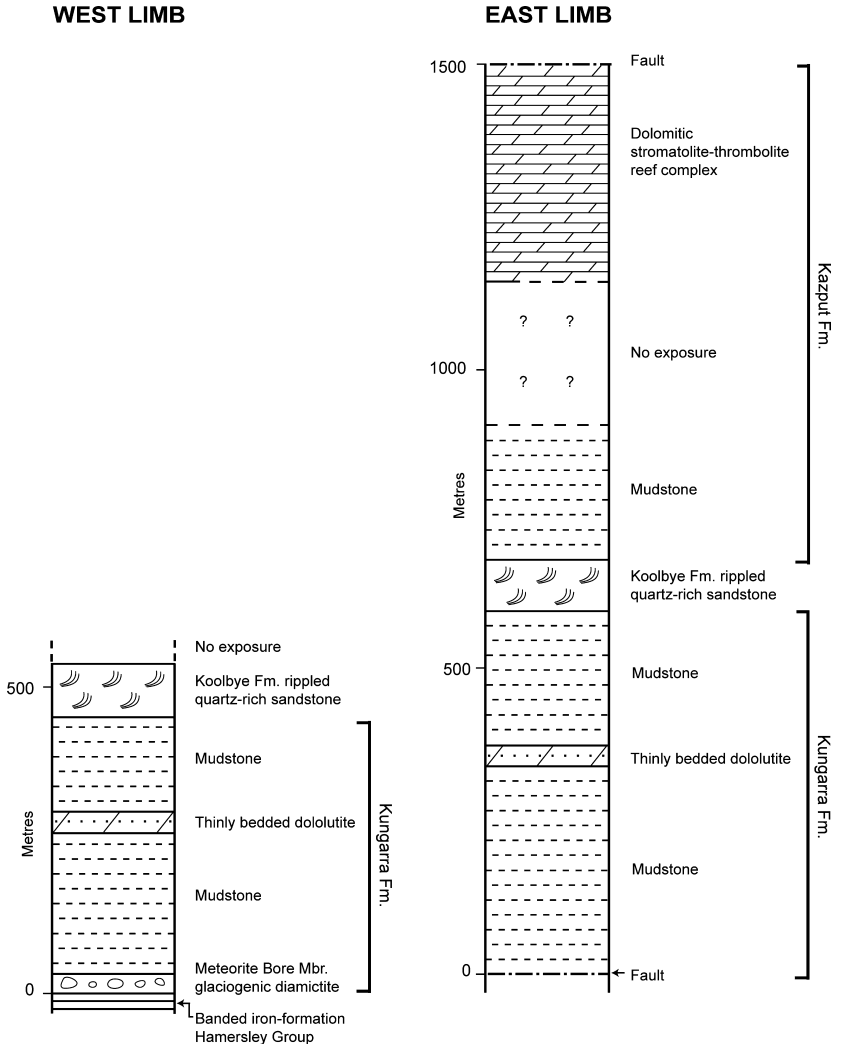

Fig. 4 West and east limbs of the Kazput Syncline. The east limb contains the Kazput Formation: the top of which hosts the stromatolite–thrombolite reef complex studied here. The west limb contains a conformable contact with the banded iron formation of the underlying Hamersley Group. Note the stratigraphic similarities on both limbs, including the Kungarra Formation and Koolbye Formation.

Structural analysis confirms that the stromatolite–thrombolite reef complex studied here belongs to the Turee Creek Group and not the younger, nearby, Duck Creek Dolomite. Four main deformational events are recognised regionally. A basal unconformity separates the Fortescue, Hamersley and Turee Creek Groups from Paleo- to Mesoarchean basement rocks. These rocks were then affected by an early set of east–west trending D_1 folds, formed as part of the Ophthalmian Orogeny that was synchronous with deposition of the Turee Creek Group at *c.* 2.43–2.40 Ga and produced a regional unconformity at the base of the Wyloo Group (e.g. locality 1 (circled) on Fig. 1; Tyler & Thorne, 1990; Rasmussen *et al.*, 2005). D_2 tilting of the *c.* 2.3–2.2 Ga Lower Wyloo Group preceded deposition of the *c.* 2.0–1.8 Ga Upper Wyloo Group, producing a third unconformity in this region. The Kazput Syncline is one of an older generation of structures ($D_{2–3}$) that also predates deposition of the upper Wyloo Group. The whole Wyloo Group (upper and lower) was then tilted during D_3, creating a fourth unconformity at the base of the Ashburton Formation. Finally, a set of regional scale, upright D_4 folds and strike-slip faults trending north-west–south-east affected the whole of the stratigraphy, including the younger Duck Creek Dolomite and Ashburton Formation, occurring synchronously with deposition of the Ashburton Formation at *c.* 1.78 Ga (e.g. Evans *et al.*, 2003). The Duck Creek Syncline is one such D_4 structure and has strike-slip faulted limbs that are offset in a manner characteristic of buckling (e.g. dextral on the eastern limb of this north-west-plunging syncline). The simple fold style of deformation (e.g. Fig. 1), and dominantly strike-slip nature of fold-related faulting in the region does not support an origin of the reef complex studied here as a fault sliver of the Duck Creek Dolomite. Given the relatively gentle westerly dips of units, an origin of the studied units as a fault slice would require either >16 km of normal displacement on a < 10° west-dipping fault, or >10 km of normal displacement on a moderately east-dipping fault, but in either scenario, the absence of associated underlying (lower Wyloo Group) or overlying (Ashburton Formation) strata, respectively, precludes such fault displacements and there is no evidence of these magnitudes of normal fault movement anywhere in the area (Figs 1 and 2). Strike-slip fault displacement of a sliver of the Duck Creek Dolomite is similarly unviable, as there are no faults that propagate through continuously from the Duck Creek Dolomite to the studied unit. Furthermore, it is clear from the map pattern and cross section in Fig. 1 that the Duck Creek Dolomite forms a structurally simple, continuous unit around the Duck Creek Syncline, whose north-eastern limb overlies older folds of older lithology: the underlying, stratigraphically older, Turee Creek Group – including the Kazput reef complex studied here – forms a continuous unit with a distinctly different map pattern controlled by the older generations of folding.

The Kazput reef complex is continuous along strike for approximately 15 km north-west–south-east and reaches a maximum thickness of approximately 350 m, with an average dip of 37° SW (darker blue in Fig. 2). It consists of a well-preserved succession of dolomitic microbialites, thinly bedded fine-grained carbonate, minor shale and thinly bedded ironstone with black chert. The reef complex hosts a diverse range of stromatolite morphology including stratiform, dome, club and branching columnar-shaped stromatolites, as well as an extensive unit of clotted (thrombolite-like) microbialite.

Five lithostratigraphic facies associations (A–E) have been established from a correlation of the 11 measured transects of the dolomitic stromatolite–thrombolite reef complex (Fig. 5). These associations are based on differences in observed lithology and variation in microbial morphology across stratigraphy. Association A is the oldest, at the base of the reef, and predominantly consists of thinly bedded dololutite to dolarenite, with local dome-shaped stromatolites. Association B is characterised by a diverse range of frequently interchanging microbial morphologies, including branching columnar stromatolites, oncolites, thin beds of thrombolite-like microbialite and a unique type of horizontally branching stromatolite, as well as thinly bedded dololutite to dolarenite. Columnar and club-shaped stromatolites dominate Association C, whereas Association D represents a thick section (up to 40 m of continuous vertical outcrop) of clotted (thrombolite-like) microbialite. Association E, at the stratigraphic top of the complex, primarily consists of thinly bedded dololutite and dolarenite, with minor grey shale, black chert and thinly bedded ironstone: there are no microbial textures or morphologies within Association E.

Regional deformation has minimal influence on the Kazput reef complex, other than minor faulting, and there is no penetrative strain. One fault is perpendicular to strike between Transects 9 and 1. Another possible fault zone, which runs parallel to strike at the base of Transects 9 and 2, appears to have caused local small-scale (1–2 m) repetition of stratigraphy. However, these faults do not substantially impact the stratigraphy of the reef complex; the entire sequence dips uniformly to the south-west, and distinct facies associations can be identified along strike (Fig. 5).

Facies Association A

Facies Association A is between 5 and 55 m thick, but the lower contact is not exposed, and thus, the full thickness is unknown. This facies association is characterised by thinly bedded dololutite and dolarenite alternating on a millime-

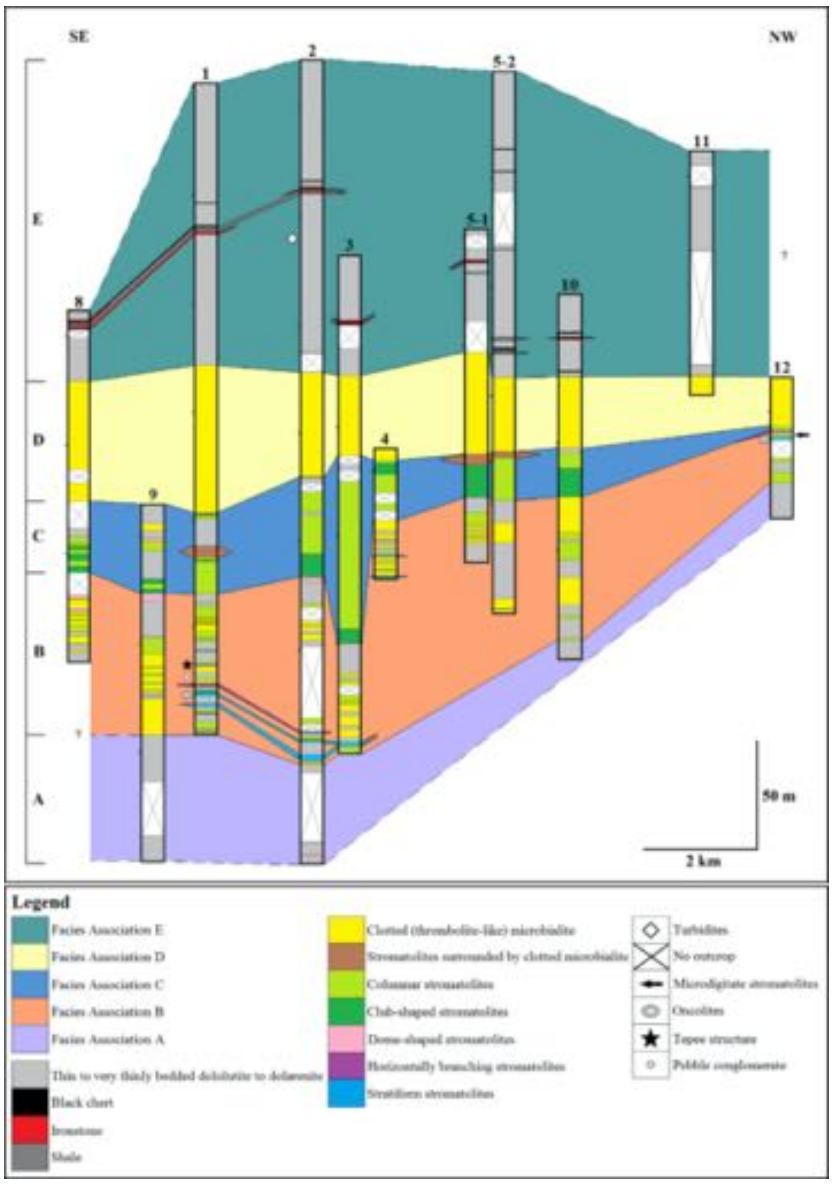

Fig. 5 Correlation of lithostratigraphic sections across the 11 measured transects of the Kazput stromatolite–thrombolite reef complex. Coloured units within the columns represent different microbial morphologies and lithological units, as per the legend; symbols indicate distinct sedimentary and microbial textures. Coloured Facies Associations A-E provide correlation between columns – dashed lines indicate inferred boundaries. Sections 6, 7 and 13 are omitted, due to lack of continuous outcrop.

tre to centimetre scale (Fig. 6A). Broad, low amplitude dome-shaped stromatolites, on average 30 cm wide and 15 cm high, were observed over a thickness of approximately 50 cm within Transect 2, towards the top of the association (Fig. 6B).

Facies Association B

Facies Association B ranges from 25 to 85 m thick, with an average thickness of 60 m. Association B consists of frequently interchanging units of columnar and stratiform stromatolites, as well as a unit of oncolites and a bed of large, horizontally branching stromatolites. A thin unit of pebble conglomerate and a large-scale tepee structure were also identified within this association, as well as minor dome-shaped stromatolites, thin units of clotted (thrombolite-like) microbialite, and thin (<20 cm) units of thinly bedded dololutite and dolarenite.

An abrupt change in stromatolite morphology is observed within Transect 2, at the disconformable boundary between Facies Associations A and B. A unit of eroded dome-shaped stromatolites (approximately 40 cm wide by 10 cm high) is overlain by a 10-cm-thick unit of dololutite, marking the uppermost point of Association A. This is followed by a unit of branching columnar stromatolites, which measure approximately 15 cm wide by 25 cm high and mark the lowermost unit of Facies Association B (Fig. 6C). Stratigraphically just above this abrupt change is a distinct sequence of microbialite morphologies, observed only in Transects 1 and 12. This sequence consists of a

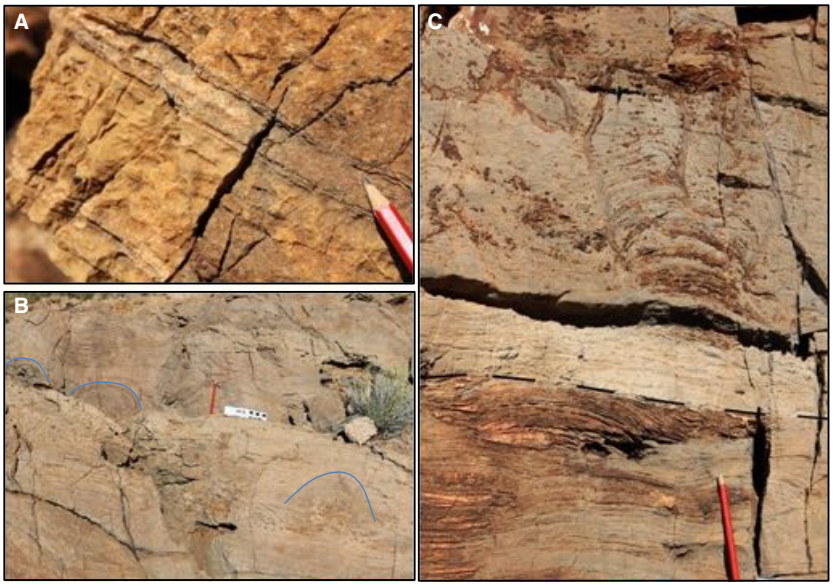

Fig. 6 (A) Alternating dololutite and dolarenite layers in Facies Association A. (B) Broad, dome-shaped stromatolites of Facies Association A in cross-sectional view (outlined in blue). (C) Contact between Facies Associations A and B; a dome-shaped stromatolite in the top of Facies Association A (just above left of pencil) is eroded (dashed black line) and overlain by dololutite with a branching, columnar stromatolite of Facies Association B on top.

16–29 cm thick bed of oncolites, followed by thin, alternating units (0.2–1.60 m thick) of tightly packed columnar and stratiform stromatolites, overlain by an approximately 1.5-m-thick unit of large tightly packed columnar stromatolites with horizontal branches.

Columnar stromatolites

Columnar stromatolites range in size from 3 to 30 cm wide and 10 to 120 cm high. Outcrops of columnar stromatolites are tightly packed, with little sediment between each column. Intercolumnar sediment generally consists of non-layered, cream-coloured dololutite–dolarenite. The synoptic relief of columnar stromatolites ranges from approximately 2–7 cm, but can locally reach up to 15 cm. Many columnar stromatolites exhibit distinctive silicified laminae and column margins (Fig. 7A).

A characteristic feature of the columnar stromatolites is the presence of convex, fine-scale microbial laminations. In thin section, these stromatolites are distinguished by alternating coarse-crystalline sparry dolomite and dark microcrystalline (micritic) layers. The finer-grained laminae are defined by clots of kerogen (see 'Raman Spectroscopy' section and Figs 7B,C), giving a distinct grey/blue hue to the stromatolites in outcrop and contrasting dramatically with the cream colour of the intercolumn non-kerogenous sediment. In thin section, columnar stromatolites reveal a distinctive texture consisting of a coarse, elongated fabric of carbonate crystals. These crystals cut the curved stromatolite laminae at 90°, regardless of the position on the stromatolite (Fig. 7D). For example, the edge of the columnar stromatolite in Fig. 7E is characterised by coarse-grained, elongated carbonate crystals that extend out, near horizontal, towards the boundary of the stromatolite and its contact with intercolumn sediment. The contrast between the microbial fabric of the stromatolites and the intercolumn sediment is clearly visible, demonstrating the syn-depositional nature of the fabric within the stromatolites and the negligible effects of metamorphic recrystallisation (e.g. Jahnert & Collins, 2012).

Stratiform stromatolites

Stratiform stromatolites are characterised by weakly undulating laminations and secondary precipitation of white-grey quartz parallel to bedding (Fig. 8A). Units of stratiform stromatolites range in thickness from 0.20 to 2.40 m. In thin section, stratiform stromatolites consist of alternating layers of light-coloured medium-grained, and dark-coloured fine-grained (micritic) layers, 0.1–0.3 mm thick (Figs 8B–D). In some areas, the alternating layers are well defined and a distinct boundary is observed. In other areas, however, there is a gradational boundary between layers, with a transition between medium and very fine-grained crystals (Fig. 8D). Stratiform stromatolites lack the penetrating, crosscutting, coarse-crystalline fabric identified in the columnar stromatolites.

Oncolites

Oncolites (type SS, as defined in Logan *et al.*, 1964) are only found in Association B, in Transects 1 and 12, within units of stratiform stromatolites. Oncolite beds are 16–29 cm thick and are located just below the horizontally branching stromatolites. On average, the oncolites are 20 cm wide and 10 cm high; some oncolites appear completely symmetrical, whereas others have a thicker build-up of layers on the top than on the bottom (Fig. 9A). This is significant because it means that these are microbially precipitated structures and not abiogenic concretions; they most likely formed in an environment with moving water.

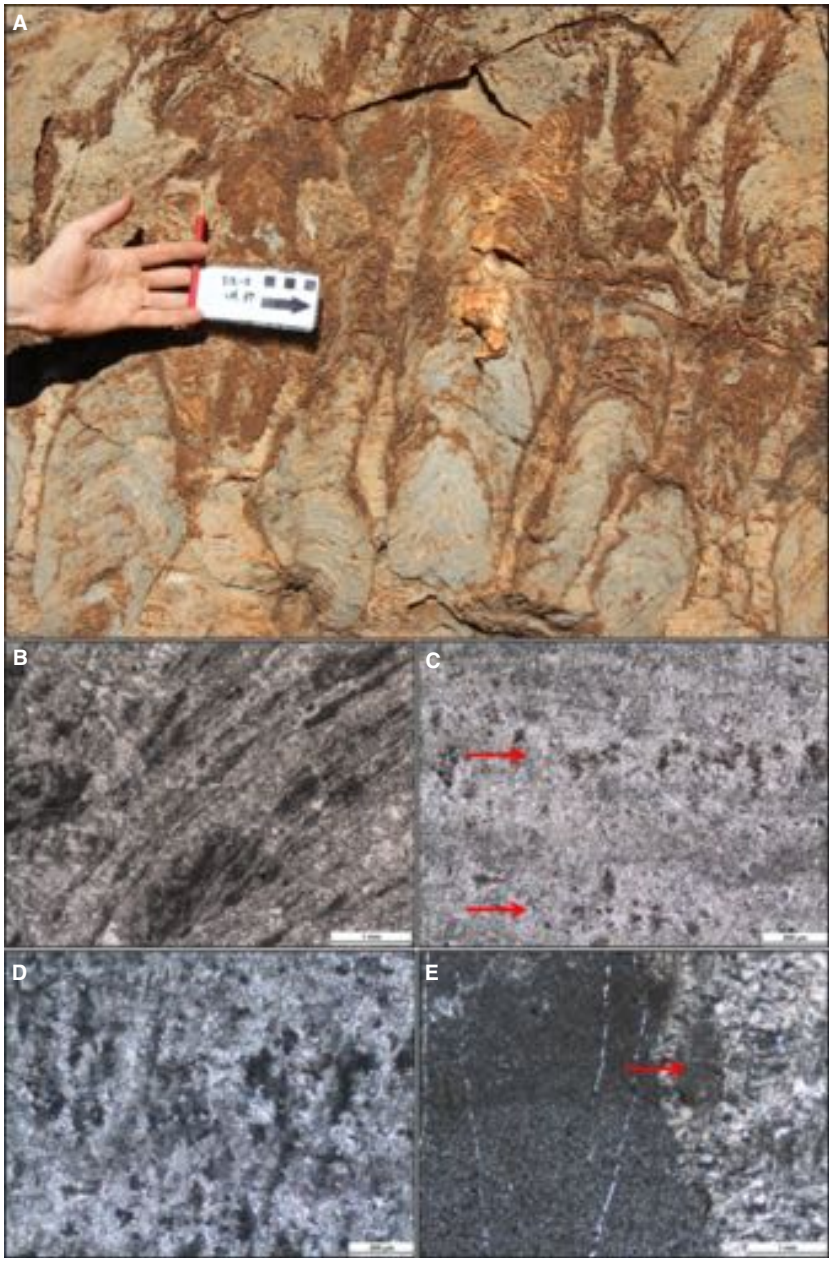

Fig. 7 (A) Representative cross-sectional view of typical columnar stromatolites in Facies Association B, exhibiting distinctive silicified laminae and column margins. (B) Plain-polarised light (PPL) view of columnar stromatolite in Facies Association B, showing alternating layers of very fine, darker (kerogenous) material and fine to medium, lighter crystalline carbonate. (C) PPL view of columnar stromatolite showing faint organosedimentary laminae running from left to right, defined by clots of kerogen (arrows). (D) Cross-polarised light (XPL) thin section view of 7C, revealing elongated carbonate crystals growing perpendicular to, and through, organosedimentary laminae. (E) XPL showing contact between bedded dololutite on the left and columnar stromatolite on the right, with a fenestra (window) in between (arrow). The stromatolite is characterised by a radiating, crosscutting dolomite crystal fabric. Note that the change in sediment colour that defines bedding on the left hand side can also be observed at the bottom of the fenestra, along the rim of the stromatolite, indicating that the crystalline fabric of the stromatolite probably preceded sediment infill and was not the result of post-depositional overprinting.

In thin section, the kerogenous and non-kerogenous laminae are easily distinguishable on the curved lateral edge of an oncolite (Figs 9B,C). The darker laminae are micritic and contain remnant kerogen (see 'Raman Spectroscopy' section), whereas the lighter laminae consist of fine to medium-sized carbonate crystals. As with stratiform stromatolites, oncolites in thin section lack the elongated crosscutting crystal fabric described within the columnar stromatolites.

Microdigitate stromatolites

Microdigitate stromatolites (Hofmann & Jackson, 1987) are observed over an 8-cm-thick unit, situated between the oncolites and the horizontally branching stromatolites in Transect 12. The microdigitate stromatolites are very tightly packed, are approximately 5 cm high and have columns typically only 3–4 mm wide that branch only at the top (Fig. 9D). Synoptic relief is very low in these stromatolites (<1 mm) and the intercolumn sediment is micritic.

Horizontally branching stromatolites

A distinctive stromatolite form was observed in Transects 1, 2 and 12. These stromatolites have a unique morphology consisting of a number of horizontal lobate branches that cap large, branching columnar stromatolite systems,

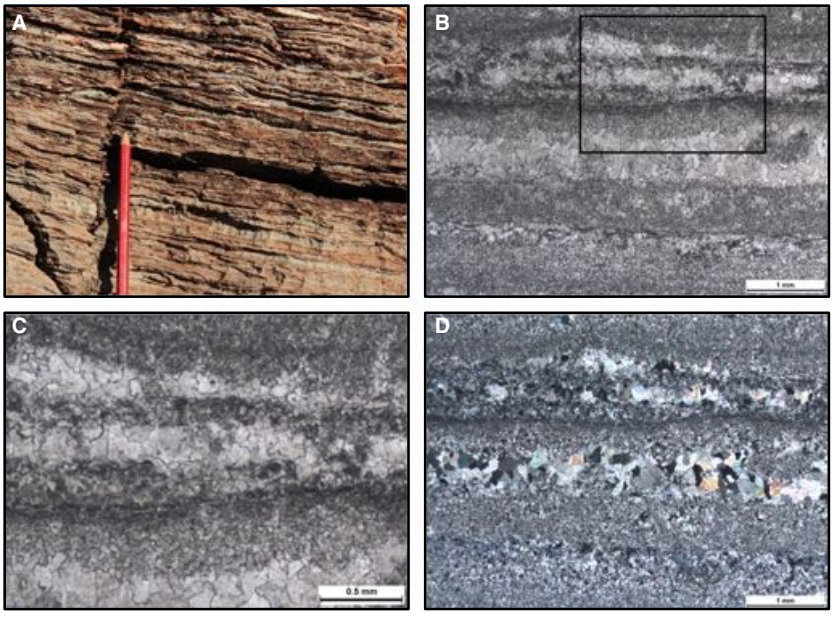

Fig. 8 (A) Stratiform stromatolites of Facies Association B, in cross-sectional outcrop view. (B) Thin section (PPL) showing variation between light, more coarsely crystalline layers, and dark, micritic layers. The black box represents the position of 8C. (C) Detail of 8B showing the contact, and the colour and crystal size variations, between layers. (D) XPL view of 8B, highlighting that each layer is characterised by different sized crystals, ranging from medium, to fine, to very fine.

which extend over 1.5 m in height (Figs 10 and 11). The base and middle part of these stromatolite systems comprise of upwardly branching columnar stromatolites, while the top 40 cm of these structures consist of stromatolites with horizontally extending branches, at right angles to the main columnar body (i.e. parallel to bedding). The horizontally extending branches are encased around the top by broad dome-shaped stromatolites (see top of Figs 10 and 11).

Both the lower columnar stromatolites and the horizontal branches contain convex laminations and have low synoptic relief, only 6–8 cm and 1–2 cm, respectively. The horizontal branches are approximately 2.5 cm high (wide) and 10 cm long and commonly curve up slightly at the tips, producing a horn-like shape (Fig. 12A). These lateral branches are characterised by silicified edges, which form as a series of elliptical to spheroidal siliceous 'balls' (bubbly or frothy-looking texture: Fig. 12B).

Each individual horizontally branching stromatolite system is immediately adjacent to its neighbour and each commences lateral branching at the same height. These stromatolite systems are tightly packed and continuous within a single bed, extending for approximately 30 m along strike in Transects 1 and 2, and approximately 20 m along strike in Transect 12. The way in which these beds terminate along strike was not observed due to lack of exposure.

Pebble conglomerate

A thin unit of pebble conglomerate, approximately 0.52 m thick, in Transect 1 consists of a range of clast sizes, including flat subrounded siliciclastic pebbles approximately 30 mm wide, and small well-rounded granules, 1–3 mm in diameter (Fig. 12C). The pebble conglomerate overlies a unit of 20-cm-high columnar stromatolites and fills the intercolumn sediment space between these stromatolites with scattered, well-rounded granules.

Tepee dewatering structures

A large-scale dewatering structure was observed within stromatolitic carbonates and bedded dolarenite–dololutite in the middle part of Association B. This structure consists of disrupted and tilted bedding, a small-scale dewatering structure (45 cm high by 25 cm wide; Fig. 12D) and sediment-filled cavities. In the lower part of the structure, blocky disrupted bedding cuts through a 55-cm-thick bed of silicified microbialite, and open spaces are locally infilled by thinly bedded dololutite. At the top of the structure, a 30-cm-thick unit of mm-cm bedded jaspilitic quartz is upwardly flexed and pierced by a 25-cm-wide vertical vein of medium to coarse-grained carbonate, which extends downwards for approximately 5 m. This represents a large-scale dewatering, or tepee structure (Fig. 12E).

Clotted (thrombolite-like) microbialite

Clotted (thrombolite-like) microbialite has a distinctive texture defined by irregular clots, 2–10 mm in diameter. These clots consist of a central core of fine-grained (<1 mm grain size), dark grey/blue to dark brown-weathering dolomite that is surrounded by a light beige-coloured, coarse-grained (1–2 mm grain size) cement. In Facies Association B, this microbialite is observed in units up to 20 cm thick. These units lack any internal stratification and occur interbedded with units of thinly bedded dololutite and dolarenite. Clotted microbialite is described in further detail in Facies Association D, where it is observed over a much larger scale.

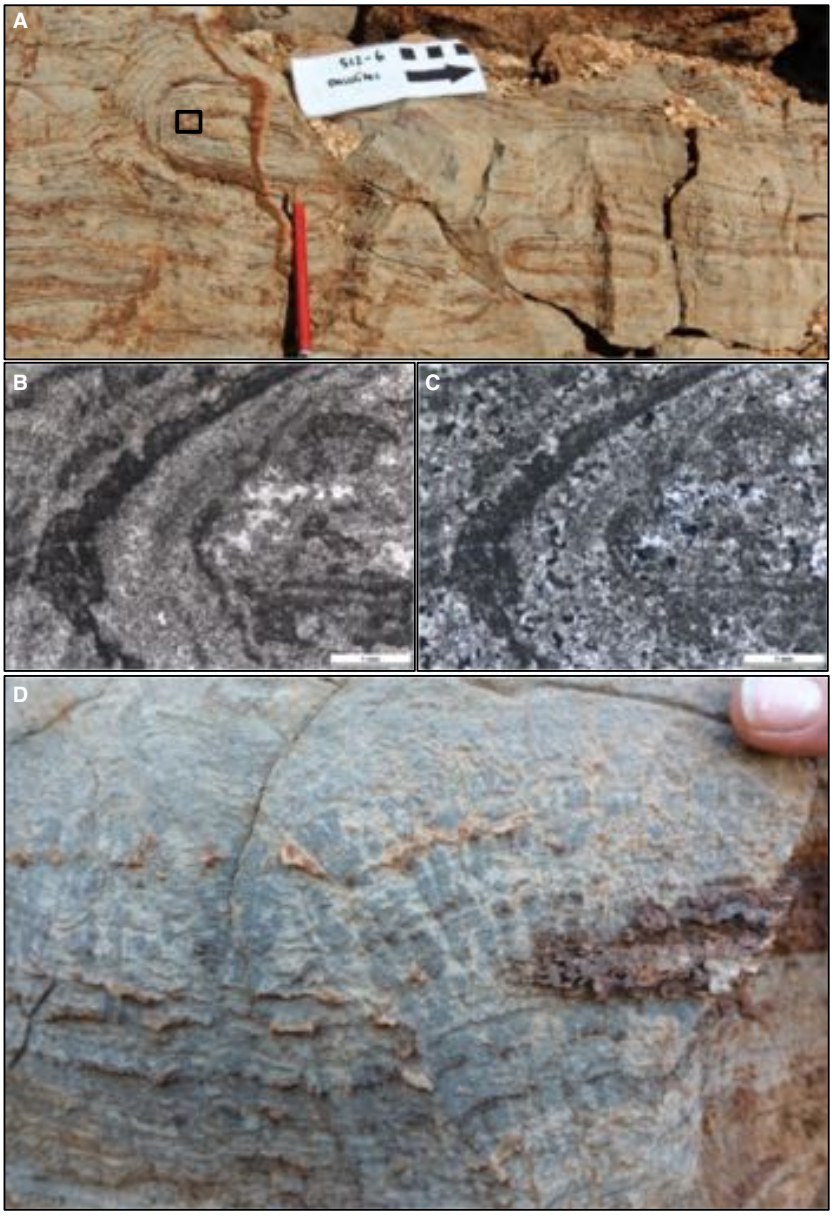

Fig. 9 (A) Oncolites of Facies Association B, in cross-sectional outcrop view, highlighting a thicker build-up of laminae on the tops of oncolites. The black box represents the position of (9B,C). (B) Lateral edge of an oncolite in PPL, showing clear variations between kerogenous (darker) and non-kerogenous laminae. (C) Same view as 9B, in XPL, highlighting different crystal sizes between layers. (D) Microdigitate stromatolites of Facies Association B, from Section 12.

Facies Association C

Spanning 5–90 m, and on average 20 m thick, Facies Association C predominantly consists of large, tightly packed columnar and club-shaped stromatolites.

Columnar stromatolites

Columnar stromatolites are generally similar to those described in Facies Association B, ranging from approximately 2–20 cm wide and 20–60 cm high. However, many columnar stromatolites in Facies Association C display upward branching and are typically dark grey/blue in colour and very densely packed, with a limited synoptic relief (5 cm on average) (Fig. 13A). The boundary between stromatolite and sediment is well defined, and there is minimal sediment between each column, with an observed ratio of approximately 75% stromatolite to 25% sediment.

The intercolumn sediment is composed of dololutite and dolarenite that is characteristically well sorted, fine-grained and lacks visible bedding in outcrop (Fig. 13B). In thin section, the sediment grains range in size from 70 to 100 micrometres (μm) and are well rounded to subhedral (Fig. 13D). The texture of the sediment is very similar to the sediment between stromatolites in Facies Association B and contrasts sharply with the internal fabric of columnar stromatolites in Fig. 7B–E.

Fig. 10 A horizontally branching stromatolite system in vertical outcrop, 1.5 m high, from Facies Association B. Note the upwardly branching nature of the columnar stromatolites in the lower two-thirds of the system and the horizontal branches in the upper one-third of the system, where they are partly silicified (dark, mottled brown). The black box shows the position of Fig. 12B.

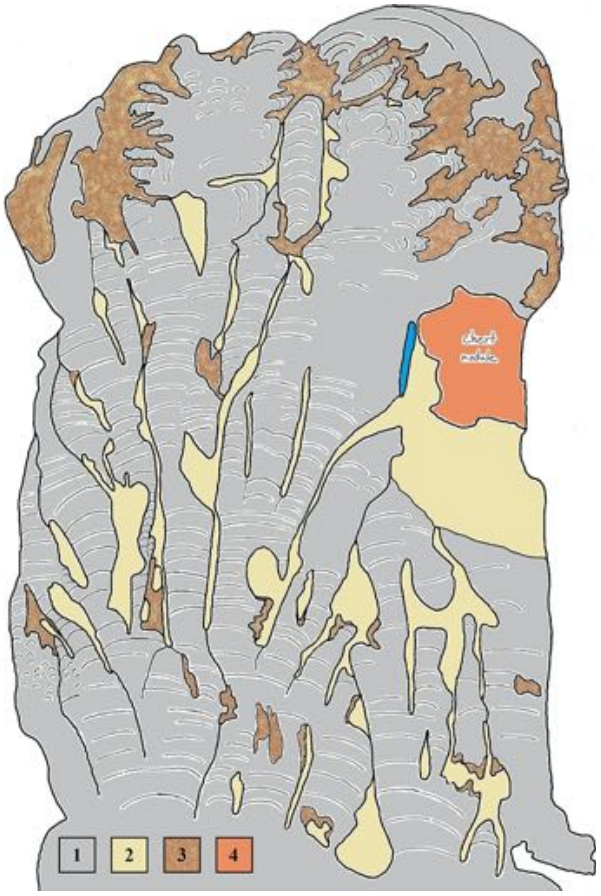

Fig. 11 Sketch of the horizontally branching stromatolite system from Fig. 10. Note the sideways 'branches' at the top of the system. 1 – stromatolite, 2 – fine-grained sediment, generally without bedding, 3 – silicified stromatolitic margins, 4 – chert nodule. The blue colour is a pen for scale.

Club-shaped stromatolites

Club-shaped stromatolites most commonly occur at the base of Association C. These 15- to 30-cm-high stromatolites are characteristically wide at the top (10–30 cm), and narrow towards the base (4–5 cm) (Fig. 13C). They have a low average synoptic relief of approximately 2 cm, and rarely branch. Intercolumn spaces are generally narrow and filled by tan-coloured dololutite.

Facies Association D

The dominant component of Facies Association D is a unit of clotted, thrombolite-like, microbialite, which occurs over an average thickness of 40 m (Fig. 5). This type of microbialite is not laminated, but consists of clots, which are irregular in size and shape, surrounded by coarse, dolomitic framework cement. The clots range from 2 to 10 mm in diameter, are generally subspherical in shape but vary to tabular and have fine-grained dark grey/blue central cores. Clots are surrounded by a lighter, beige-coloured supporting framework, or 'rind' of coarser-grained (1–2 mm) dolomite cement (Fig. 14A). In places, infrequent thin units of dololutite (up to 10 cm thick) are interbedded with the thrombolitic microbialite.

Near the top of Association D, the randomly distributed clotty texture passes up into small, narrow stromatolites, approximately 5 cm high by 1 cm wide that show localised, crude upward-branching (Fig. 14B). These small stromatolites have very faint, convex upward internal lamination and have an unusual 'ragged' appearance of stacked lobes, giving an overall segmented appearance.

At the base of Association D in Transects 1, 5-1 and 5-2, clotty-textured microbialite encases the tops and sides of small, club-shaped stromatolites of Association C. These club-shaped stromatolites of the underlying association are approximately 16 cm high, with an average width of 14 cm at the top, narrowing to 5 cm at the base, with a distinctly elongate shape in plan view (Fig. 14C). The clotty-textured microbialite has the same appearance in

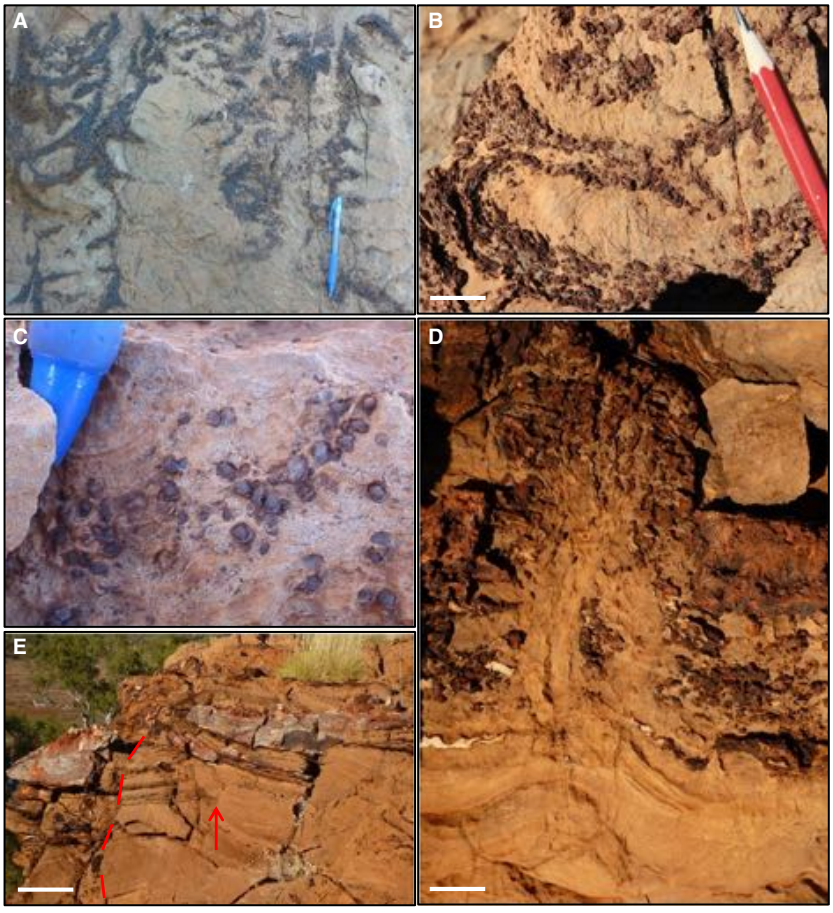

Fig. 12 (A) The top one-third of the horizontally branching stromatolite system, highlighting the slightly curved, horn-shaped horizontal 'branches'. (B) Close-up of horizontal branches, showing faint, convex outward laminations and spherical siliceous 'balls' (scale bar = 1 cm). (C) Close-up of small well-rounded silicic clasts (1–3 mm in diameter) in the pebble conglomerate, immediately overlying the horizontally branching stromatolites of Facies Association B (scale = pen tip, 0.5 cm). (D) Small tepee structure cutting through partly silicified stratiform stromatolites of Facies Association B, in cross-sectional view (scale bar = 5 cm). (E) Large-scale dewatering structure in bedded carbonate and jaspilitic chert (light grey unit near top). Note the discordant bedding beneath the jaspilitic chert (arrow) and the carbonate vein that cuts through the jaspilitic chert and underlying bedded carbonates (dashed line) (scale bar = 50 cm).

both vertical section and plan view (Figs 14C,D), with no preferred direction of elongation of the clots. No bedding, or any sort of lamination, or grading of the clots is apparent either among or within the clots. The clots are highly irregular in shape, with small projections and embayments, but most are equidimensional.

The clotted (thrombolite-like) microbialite has a striking texture in petrographic thin section. The clots are much darker than the surrounding carbonate cement and are approximately equidimensional and subspherical, with highly irregular edges (Fig. 15A,B). Subspherical clots range in size from 1 to 2.5 mm in diameter, but clots may locally be more elongate, reaching a maximum size of 3 mm by 1 mm. The clots are micritic in the centre and commonly contain highly ragged rims of darker material, interpreted to be more kerogen rich (see 'Raman Spectroscopy' and Fig. 15A,B). Each clot is surrounded by coarse dolomite cement consisting of elongated crystals, ranging from 1 to 1.5 mm in length, that radiate outward around the clot (Fig. 15C,D). The sutures between the clots show euhedral crystal tips pointing into what was a void space, but that is now filled by clear, undeformed crystals of quartz (Fig. 15E,F).

Facies Association E

Facies Association E is approximately 150 m thick and consists predominately of thinly interbedded dolarenite and dololutite (0.5 cm thick), but includes subordinate shale, bedded ironstone and black chert. All of these units extend along the entire strike length of the reef complex. There are no stromatolites or clotted microbialite textures within this association. The dololutite and dolarenite beds are composed of well sorted, very well-rounded grains. Turbidite beds, consisting of a 2- 5-cm-thick repeating sequence of dolarenite grading into dololutite with very fine bedding (Fig. 16A), were observed in Transect 2, approximately 20 m below a thin succession (0.3–5 m thick) of grey shale (Fig. 16B). The shale unit is symmetrically flanked above and below by units of thinly bedded ironstone, 0.3–1 m thick, in Transects 8, 1, 2, 3 and 5–1. The thinly bedded ironstone is composed of bedded siderite and haematite, with abundant manganese oxides (Fig. 16C). The shale-ironstone succession occurs approximately halfway through Facies Association E.

Within the ironstone units and in immediately adjacent interbedded dolarenites and dololutites are a series of black

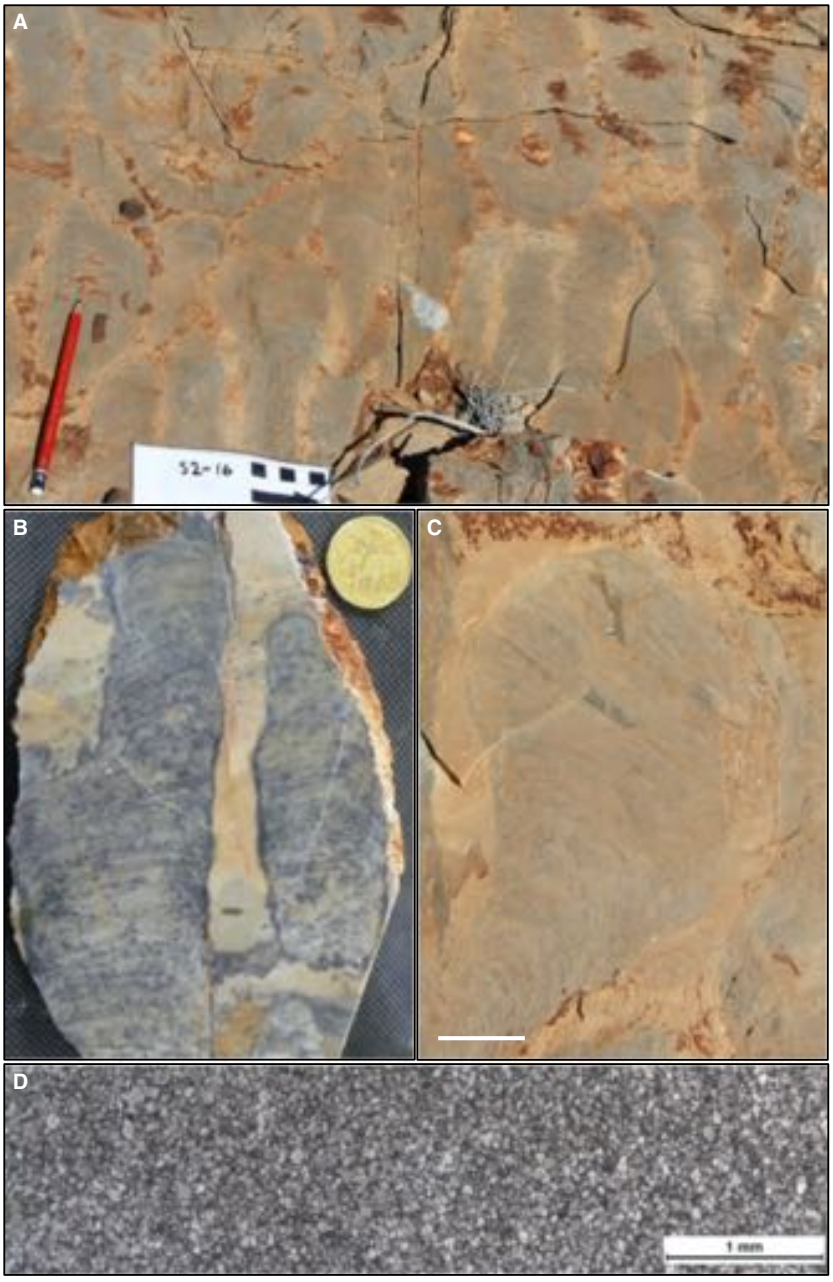

Fig. 13 (A) Tightly packed, branching columnar stromatolites of Facies Association C, ranging from 10–15 cm high and 3–7 cm wide. (B) Sample block of two columnar stromatolites, highlighting dark grey/blue laminae within the stromatolites and the non-bedded, very fine-grained intercolumnar sediment. (C) Outcrop view of club-shaped stromatolite in cross section (scale bar = 5 cm). (D) Thin section of intercolumnar sediment, from between columnar stromatolites in 13B (PPL view).

chert units consisting of continuous chert layers, disrupted lenses and nodules of black chert, and black chert cores to carbonate concretions (Fig. 16D,E). The layers vary from 1 to 10 cm thick and may be continuous along strike for 10's of metres, parallel to bedding in the dolarenite–dololutite. Nodules of black chert are typically 5 cm high by 15 cm wide, and carbonate concretions can reach up to 18 cm high by 55 cm wide.

Petrographic analysis of black chert samples reveals a texture consisting predominantly of equigranular microquartz, but also localised large spherulites, 180–550 μm in diameter (Fig. 16F). Straight contacts separate adjacent spherulites, suggesting outward growth of the silica needles from central, spaced nucleation points. Sparse, perfectly formed dolomite rhombs within the chert have approximate dimensions of 200 μm by 360 μm and display distinct growth zones (Fig. 16G).

Herringbone Cement

Herringbone cement (Sumner & Grotzinger, 1996; Bartley *et al.*, 2014) was observed in a few localities near the base of the reef complex in Facies Associations A and B. It is characterised by a distinctive chevron-like pattern and

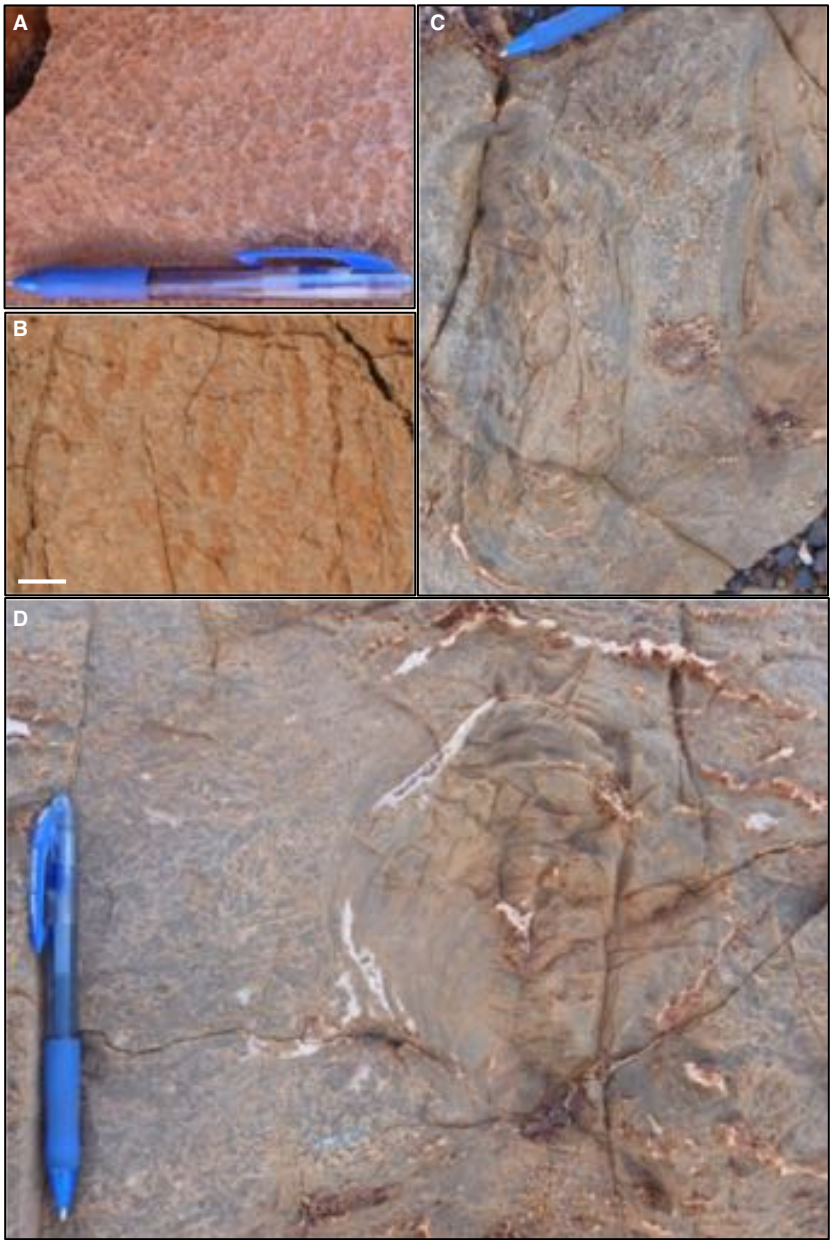

Fig. 14 Clotted (thrombolite-like) microbialite of Facies Association D: (A) outcrop view of typical clotted microbialite showing dark, fine-grained central clots and surrounding coarser-grained carbonate cement. Note the absence of any layering, or grading of clots (pen points to way-upward). (B) Small segmented stromatolites within the upper part of Facies Association D, growing upwards from, and within, clotted microbialite (scale bar = 3 cm). (C) Clotted microbialite encasing elongated stromatolites in bedding-plane view. (D) Cross-sectional outcrop view of 14C, showing clotted microbialite (from the base of Facies Association D), surrounding a club-shaped stromatolite (representing the top of Facies Association C). Clots here are highly irregular in shape and non-laminated.

occurs in layers and irregular to locally spherical patches (Fig. 17A). In thin section, this cement consists of fibrous carbonate crystals with strong vertical alignment. These crystals are approximately 1000 μm long by 120 μm wide (Figs. 17B,C).

RAMAN SPECTROSCOPY

Optical microscopic analyses of petrographic thin-section samples of microbialites from the Kazput stromatolite–thrombolite reef complex allowed for the initial identification of remnant organic material, known as kerogen (Summons & Hallmann, 2014). Kerogen in these samples has a light to medium brown-coloured, globular amorphous appearance under transmitted light. Raman spectroscopy can be a useful technique in confirming the presence of kerogen and establishing the biogenicity of samples (e.g. Kudryavtsev *et al.*, 2000; Schopf *et al.*, 2002, 2005; Marshall *et al.*, 2011). For this reason, Raman spectra of the kerogen were attained on representative thin-section samples of columnar stromatolite, oncolite and clotty-textured microbialite. The columnar stromatolite spectrum displays the major kerogen peaks centred at ~1358 cm^{-1}, known as the disorder or 'D' band (Castiglioni *et al.*, 2001), and ~1601 cm^{-1}, known as the graphitic, or 'G' band (Tuinstra & Koenig, 1970; Fig. 18). Due to strong fluores-

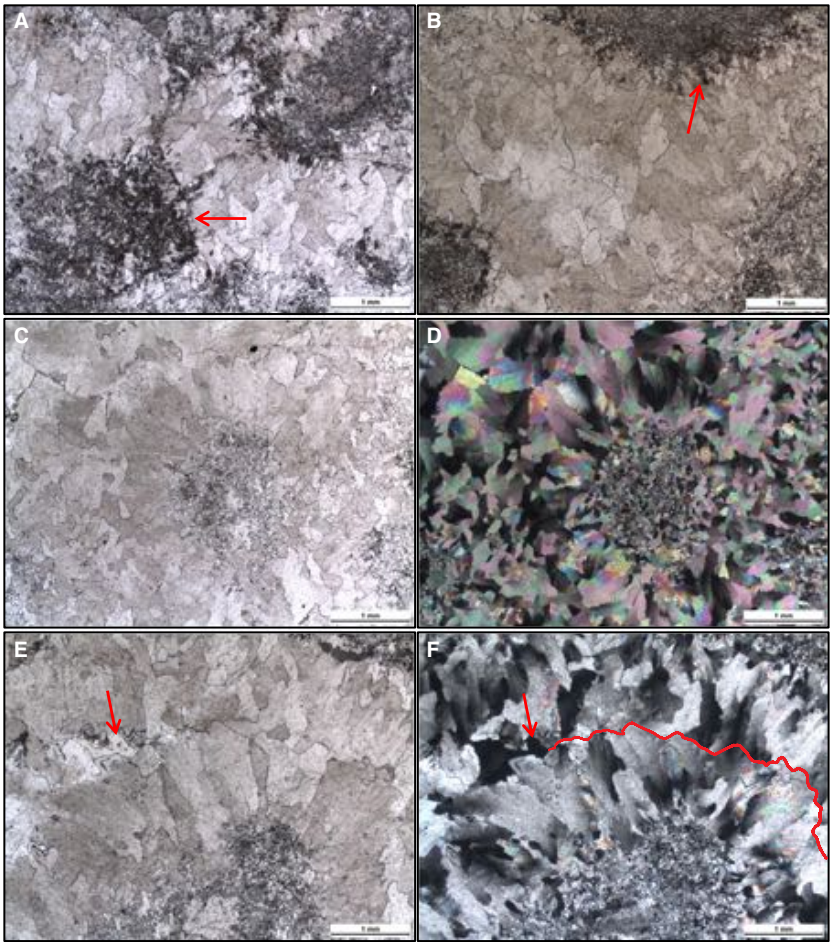

Fig. 15 Thin section images of clotted (thrombolite-like) microbialites of Facies Association D: (A) touching and (B) spaced kerogenous clots, separated by light-coloured, coarse-grained, radiating dolomite cement. Arrows highlight the more kerogen-rich and highly ragged rims of clots (PPL). (C) PPL and (D) XPL views of a single, fine-grained clot surrounded by coarse crystalline, radiating dolomite cement. (E) PPL and (F) XPL images of two spaced, fine-grained clots (lower middle and upper far right) and the radiating dolomite cements from each. These cements meet along a suture (traced in red in F) that includes a small void space (arrows) into which euhedral carbonate crystal tips extend.

cence in the oncolite and clotted microbialite samples, it was difficult to obtain as well-resolved peaks as in the columnar stromatolite. Even so, the oncolite spectrum displays similar results to the columnar stromatolite spectrum, with the D band centred at ~1334 cm^{-1} and the G band centred at ~1606 cm^{-1} (see Supporting Information). The clotted microbialite spectrum is not as well resolved as the columnar stromatolite and oncolite spectra. However, the major kerogen peaks centred at ~1326 cm^{-1} and ~1616 cm^{-1} can still be clearly identified (see supplementary data; please note that in this case, the differences in intensity (counts) between the spectra are an artefact of sample preparation and thus cannot be used as part of a quantitative comparison). Given the visually similar characteristics of the kerogenous material identified in the clotted microbialite petrographic thin section (Fig. 15A,B) as the kerogen from the other samples with more well-defined spectra (Fig. 7B–D, 9B,C), we interpret that this sample reflects kerogen as well. All three spectra show similar peak wave numbers for the D and G bands and all also display a prominent carbonate peak at ~1098 cm^{-1}.

There is no evidence in either outcrop or microscopic scale of a hydrothermal vein influence on the reef complex. Thus, the identification of microbially induced laminae and clots in outcrop, as well as kerogen in thin sections and in Raman spectra, along with a lack of evidence of late contamination by hydrothermal veins, all points to a biogenic origin of the kerogenous material, confirming the biogenicity of the microbialite samples.

CARBON AND OXYGEN ISOTOPES

Stable isotope analysis of Kazput Formation bedded dolostone reveals little variation in either $\delta^{13}C_{carb}$ or $\delta^{18}O_{carb}$ values across the unit (Fig. 19; Table 1). Values of $\delta^{13}C_{carb}$ range from 0.47 to 1.41‰ (VPDB: average = 0.68‰) in the lower, more shallow-water facies of the unit (Associations B and C), but are slightly lower (−0.22 to 0.11‰) in the deeper-water Facies Association E near the top of the succession. Values of $\delta^{18}O$ in the dolostones range from −14.8 to −9.7‰ (VPDB), having the most negative values near the top of the unit in samples that also have negative $\delta^{13}C$ values. These values are within the field of elevated fluid temperatures, likely reflecting some isotopic exchange. A positive correlation between $\delta^{13}C_{carb}$ and

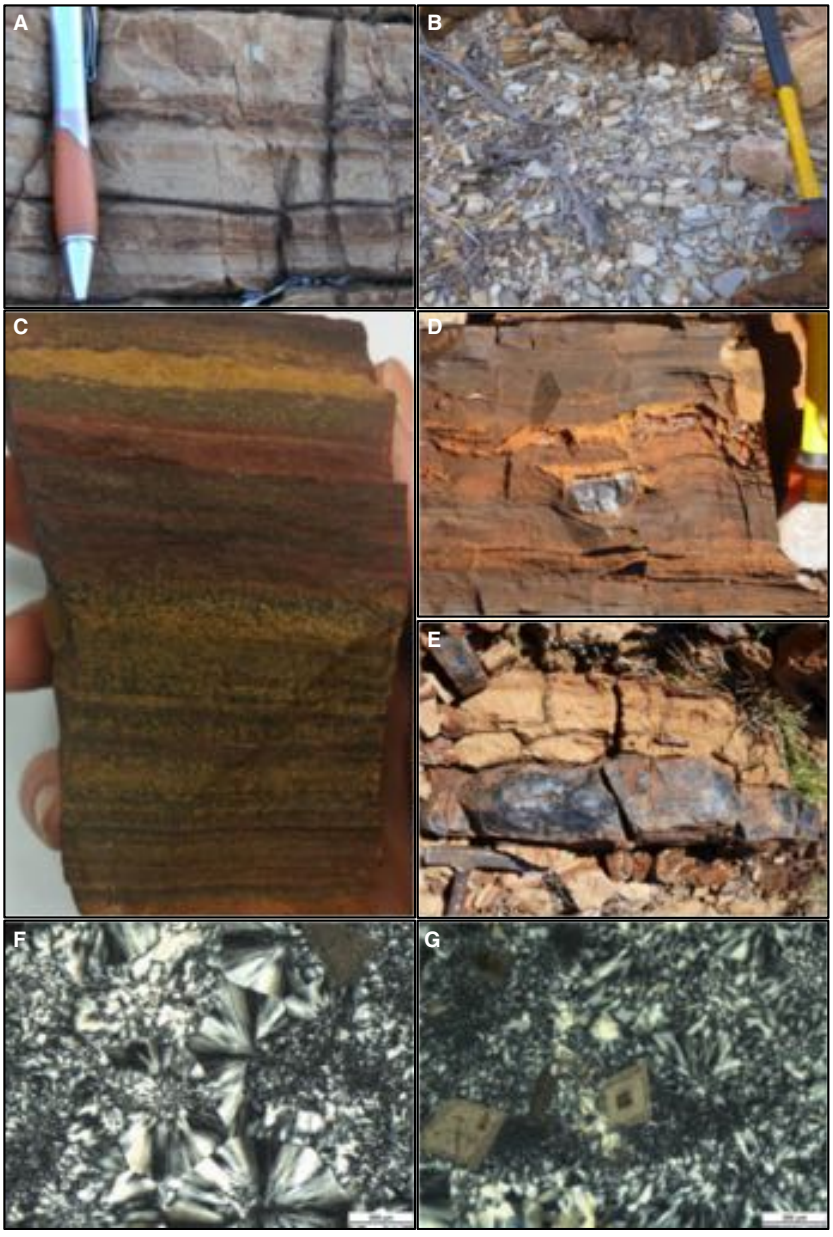

Fig. 16 Rock types of Facies Association E: (A) turbidite beds within the middle part of Facies Association E (Transect 2), showing graded bedding from dolarenite into dololutite, and planar bedding within the upper parts of graded beds. (B) Weathered outcrop exposure of the shale unit. (C) Hand specimen of ironstone unit, containing siderite (tan) and haematite (red), with abundant black spots of manganese oxide (width of sample at base = 5 cm). (D) Nodular black chert within bedded ironstone (diameter of hammer head = 5 cm). (E) Bedding-parallel black chert within bedded dololutite. Thin section (XPL) views of black chert with; (F) large spherulites, and (G) zoned dolomite rhombs.

$\delta^{18}O_{carb}$ values supports a minor degree of alteration, most likely by fluids associated with Paleoproterozoic (*c.* 2.2 Ga) metamorphism (e.g. Rasmussen *et al.*, 2005).

DISCUSSION

The *c.* 2.4–2.3 Ga Kazput Formation stromatolite–thrombolite reef described here contains features characteristic of other Paleoproterozoic microbialite reefs, including the *c.* 1.8 Ga DCD and *c.* 1.9 Ga Rocknest Formation. However, it is 300–500 Ma older than previously described examples and was formed immediately after the rise of atmospheric oxygen. In order to better understand the significance of the different morphologies and textural features documented within the complex studied here, we assess the primary nature of the preserved fabrics and compare the complex with both older and younger marine stromatolitic reefs, as described from the geological literature.

Primary vs. secondary textures

One of the common questions facing petrographic analysis of stromatolitic carbonate successions is the degree to which primary textures are preserved or overprinted by secondary recrystallization. Understanding these relationships is particularly important for determining the origin of

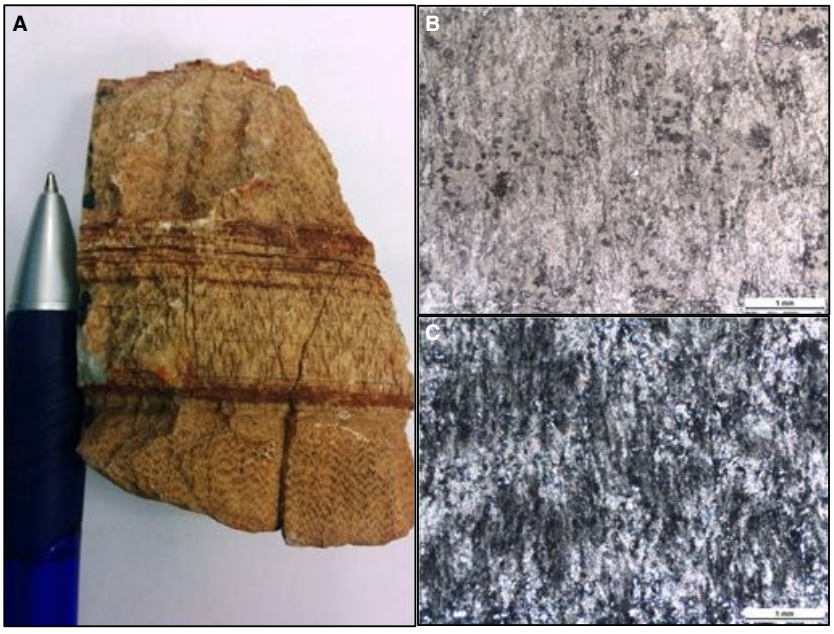

Fig. 17 (A) Sample of herringbone cement, displaying characteristic chevron pattern. (B) PPL and (C) XPL thin sections of herringbone cement showing the strong, vertical alignment of crystals: approximately 1000 μm long by 120 μm wide.

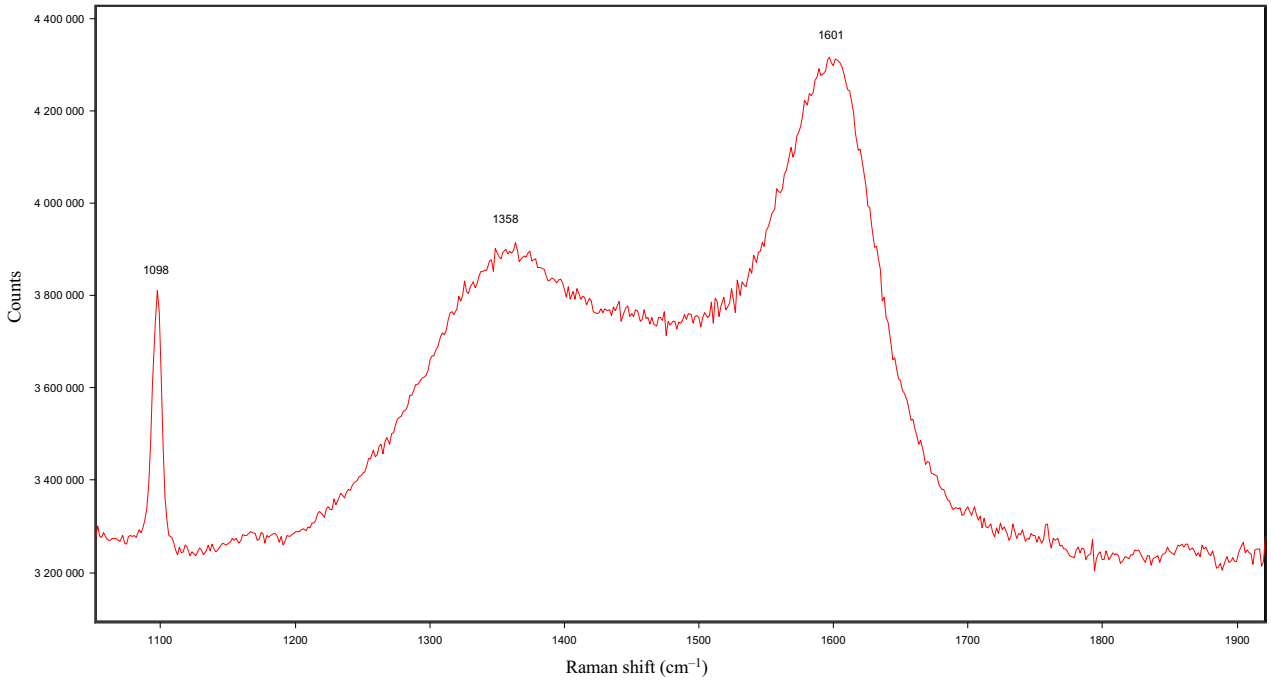

Fig. 18 Columnar stromatolite Raman spectrum exhibiting peaks characteristic of kerogen: the disorder or 'D' band (Castiglioni *et al.*, 2001) centred at ~1358 cm^{-1} and the graphitic, or 'G' band (Tuinstra & Koenig, 1970) centred at ~1601 cm^{-1}. Note the carbonate peak centred at ~1098 cm^{-1}.

the thrombolite-like microbialites described in Facies Associations B and D.

It is clear from both outcrop and thin section-scale observations that the degree of preservation in the studied reef complex is exceptional, as demonstrated by the preservation of fine lamination in stromatolites, oncolites and microdigitate stromatolites, and the clear preservation of kerogen in columnar stromatolites and oncolites.

It is possible to understand the mechanism of syndepositional crystallisation within some of the microbialites. The

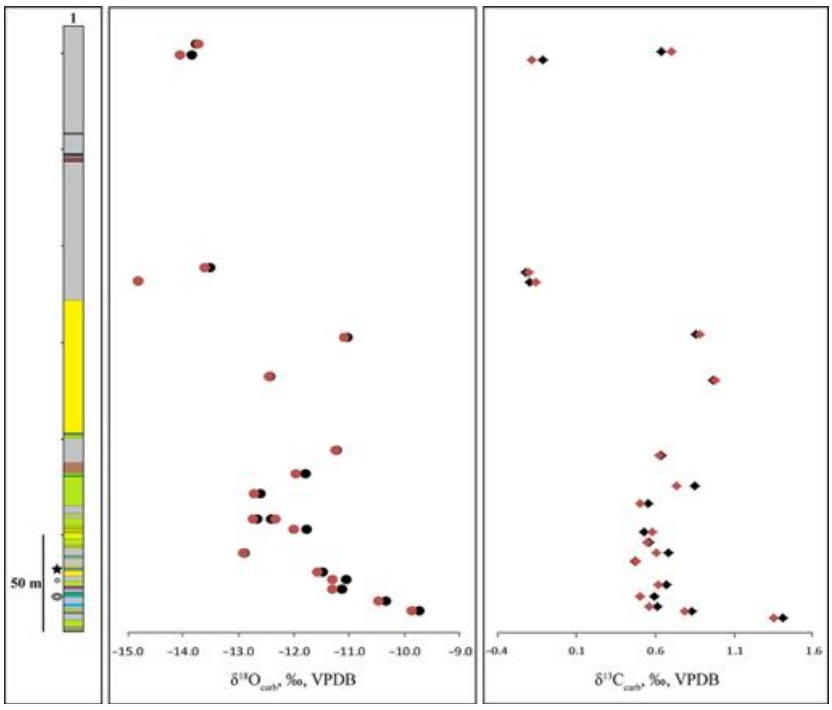

Fig. 19 Oxygen and carbon isotope values from samples along Transect 1, in reference to the Vienna Pee Dee Belemnite (VPDB) standard. Red and black symbols represent duplicate analyses. Legend for Transect 1 is in Fig. 5.

example of a finely laminated columnar stromatolite that is characterised by a fabric of coarse carbonate crystals cross-cutting the lamination is significant, as this texture sharply contrasts with the immediately adjacent, fine-grained, intercolumn carbonate sediment (Fig. 7E). That the cross-cutting texture is syndepositional is shown by a fenestra (arrow in Fig. 7E) within the margin of the stromatolite that is filled by the intercolumn sediment and even contains the bedding contact preserved within the sediment. This contrast in texture between stromatolite and intercolumn sediment shows that there has been little, or no, overprinting by late diagenetic and/or metamorphic recrystallisation.

A number of working hypotheses for the formation of the extensive unit of thrombolite-like microbialite of Facies Association D include: (i) broken up stromatolitic fragments from a storm event; (ii) tsunami/mudflow-type deposit; and (iii) primary microbialite (thrombolite) texture. We regard option 1 as improbable, as there is no evidence in either outcrop or thin sections of layering within or between the clots and the texture is observed to be continuous and homogeneous over such an extensive thickness (up to 40 m) and distance along strike (across 13 km). Option 2 is also regarded as improbable due to a lack of sorting or grading of the clotted material. Furthermore, at the very base of the unit, the thrombolite-like microbialite is observed encasing undamaged club-shaped stromatolites, which discounts a mass waste deposit origin, as the base of such a depositional unit should be strongly erosional. Rather, we propose that this clotted form developed *in situ*, as a primary microbialite (Kennard & James, 1986). The appearance of the internally clotted texture fits the most accepted definition for thrombolites (Aitken, 1967; Kennard & James, 1986; Riding, 1999) and is similar in appearance to thrombolites of the *c.* 1.9 Ga Rocknest Formation documented by Kah & Grotzinger (1992). The fine-grained centre of the clots and contrasting texture of the outer marine cements shows that there has been little or no recrystallisation and that the marine cements overgrew biologically precipitated carbonate. Thus, the formation and preservation of the thrombolite-like microbialite are considered to have been in a low-energy, low-sediment input, subtidal environment of sea water that was supersaturated in $CaCO_3$. This is based on an analogy with younger thrombolites; similar textures are formed in modern microbialite reefs by coccoid cyanobacteria, where structures are preserved by rapid microbially driven carbonate precipitation and cementation (Kennard & James, 1986; Grotzinger, 1990; Kah & Grotzinger, 1992; Jahnert & Collins, 2012).

In this proposed mode of formation, microbially induced clots would have been underpacked and just touching on random, irregular edges, causing pockets of sea water between the clots to become blocked off from the main body of sea water. Little detrital input to the system at this time would have resulted in these pore spaces remaining open, allowing for the rapid cementation of the pore space between clots, preserving the primary structures. This

Table 1 $\delta^{13}C$ and $\delta^{18}O$ values analysed from samples taken across Transect 1, in reference to the Vienna Pee Dee Belemnite (VPDB) standard. NBS is the National Bureau of Standards

Sample Name	NBS-corrected $\delta^{13}C$ (VPDB)	Standard error	NBS-corrected $\delta^{18}O$ (VPDB)	Standard error
Batch 1 (June 9, 2010)				
197463	1.412	0.002	−9.719	0.006
197464	0.833	0.002	−10.317	0.004
197465 A	0.618	0.003	−11.119	0.006
197465 B	0.597	0.002	−11.049	0.007
197466	0.671	0.003	−11.471	0.009
197467	0.473	0.003	−12.876	0.009
197468	0.687	0.003	−11.769	0.004
197469 A	0.566	0.002	−12.651	0.005
197469 B	0.533	0.002	−12.391	0.008
197470	0.558	0.002	−12.603	0.006
197471	0.851	0.003	−11.778	0.006
197472	0.643	0.003	−11.215	0.002
197473	0.970	0.005	−12.420	0.006
197474	0.861	0.003	−11.025	0.007
197475	−0.191	0.007	−14.803	0.006
197476	−0.222	0.003	−13.501	0.008
197477	−0.113	0.004	−13.836	0.007
197478	0.638	0.002	−13.756	0.005
Batch 2 (June 18, 2010)				
197463	1.355	0.003	−9.867	0.008
197464	0.789	0.003	−10.463	0.004
197465 A	0.566	0.003	−11.296	0.009
197465 B	0.504	0.006	−11.297	0.007
197466	0.619	0.001	−11.570	0.007
197467	0.479	0.002	−12.901	0.004
197468	0.608	0.002	−12.000	0.010
197469 A	0.550	0.005	−12.739	0.002
197469 B	0.586	0.003	−12.314	0.003
197470	0.506	0.003	−12.711	0.007
197471	0.735	0.005	−11.951	0.010
197472	0.626	0.004	−11.233	0.006
197473	0.980	0.003	−12.439	0.005
197474	0.887	0.002	−11.077	0.005
197475	−0.156	0.004	−14.796	0.006
197476	−0.199	0.003	−13.612	0.008
197477	−0.181	0.002	−14.049	0.005
197478	0.708	0.001	−13.712	0.007

The letters A and B refer to 2 individual samples being collected from the one location.

model is supported by the fact that primary textures are clearly preserved, with little or no recrystallisation, throughout the clotty-textured microbialite, as evidenced by the radiating dolomitised cement and irregular nature of the central clots.

Facies analyses

A representative lithostratigraphic column of the entire study area was constructed from the individual transects (Fig. 20). Characteristics of the five lithostratigraphic facies associations (A-E; described below) were used to estimate relative water depths at the time of deposition.

Facies Association A

There is insufficient evidence from the thinly bedded dololutites and dolarenites of this association to draw direct conclusions about the depositional environment, as this association could represent either a low-energy, shallow-water lagoon, or a moderately deep to deep water marine environment. However, a relatively deep water environment for the bulk of this association is preferred, as there is a complete lack of current indicators, or storm deposits. As such, we infer deposition below storm wave base. A relatively deeper-water setting is supported by the presence of a moderate to deep water environment lying stratigraphically below the reef complex, consisting of fine-grained siliciclastics and very thinly bedded dololutite (Fig. 3). In contrast, a relatively more shallow-water environment is suggested for the top of Facies Association A, based on the presence of the low amplitude domical stromatolite horizon, which most likely lay within the photic zone.

Facies Association B

There is a close spatial relationship between key units within the middle of Facies Association B. These key units include stratiform stromatolites, oncolites, horizontally branching stromatolites, a thin unit of pebble conglomerate, bedded jaspilitic quartz and a large-scale dewatering structure. All of these individually, but particularly when considered collectively, infer a very shallow water, to periodically exposed, environment of deposition. For example, modern smooth microbial mats found in Shark Bay, Western Australia, may be used as analogues for the stratiform stromatolites in the reef complex studied here, as these microbialites characteristically develop in the 'spray zone' of the supratidal zone (Donaldson, 1976; Hoffman, 1976; Playford & Cockbain, 1976). Similarly, oncolites are formed in periodically highly turbulent waters, where wave-action and/or storm events keep the sea floor in motion (Gebelein, 1976). This periodic movement prevents the microbes from consolidating into a mat structure and creates the characteristic encapsulating laminae. Due to the mode of formation, it is generally accepted that oncolites also occur in a shallow-water, intertidal environment (Donaldson, 1976; Gebelein, 1976).

The horizontally branching nature of stromatolites from this facies association has not, to our knowledge, previously been described in the geological literature. The closest comparable stromatolite form is the *c.* 1.1 Ga Jacutophyton, which is characterised by a central column of conical laminae, with angled branches extending out at 45° from the sides of the central structure (Walter, 1972; Kah *et al.*, 2009). The branching cones of Jacutophyton are approximately 5 cm wide and up to 50 cm long, extending along the entire height of the central cone. The central cone consists of conical laminations with high synoptic

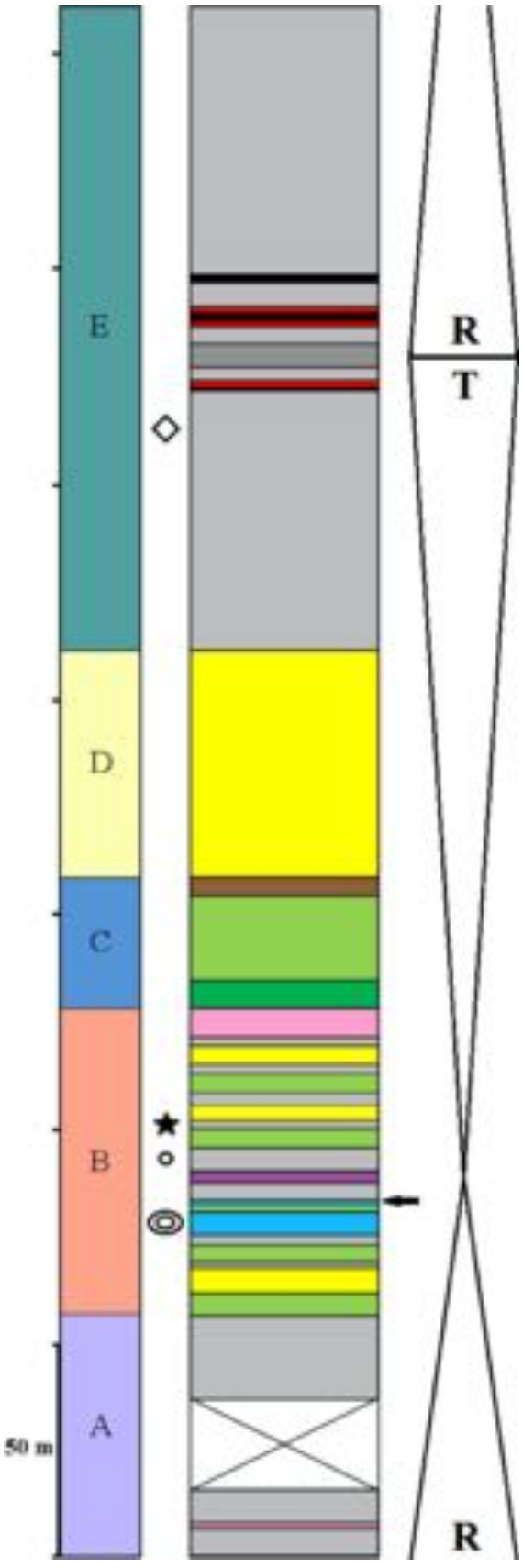

Fig. 20 Representative lithostratigraphic column for the studied ridge, compiled from the measured sections presented in Fig. 5. Associations A–E are illustrated on the left and on the right the regression (R) and transgression (T) sequences. For legend, refer to Fig. 5.

relief, whereas the branches consist of convex laminations and have a synoptic relief of only 4–5 cm. Although Jacutophyton and the horizontally branching stromatolites studied here both consist of a main body and sideways branches, key differences between the two include: the conical body and branches at an angle of 45° in Jacutophyton, versus the columnar form of the unit described here, where the sideways branches are at 90° to the main body. The horizontally branching stromatolites described here also have branches that curl up slightly at the tips, contrasting with the straight branches of Jacutophyton. However, the sideways branches of both of these morphologies are best explained as having arisen from a drop in sea level, to below the height of the main vertical 'core' of the stromatolites, indicating growth of the inclined to horizontal branches just below the water–air interface in response to restricted vertical growth space (Kah *et al.*, 2009). A similar feature can be observed on modern intertidal stromatolites at Shark Bay that have been partially exposed by relative sea level fall. These club-shaped structures have a dead cap on top and a rind of new stromatolite growth around the sides (Playford *et al.*, 2013).

Thus, we suggest the close stratigraphic relationship of a variety of features in the middle of Facies Association B indicates a period of very shallow water, to periodically exposed conditions, likely an intertidal zone (e.g. Gandin *et al.*, 2005). Being in the middle of Association B, this sequence represents the top of a shallowing-up succession (regression) from the preceding Facies Association A and underlying siliciclastics, and the base of an overlying deepening-up (transgression) succession.

Facies Association C

Facies Association C is characterised by columnar and club-shaped stromatolites, suggesting deposition in a lower-intertidal to shallow subtidal environment (Donaldson, 1976; Hoffman, 1976; Playford *et al.*, 2013). This represents a progression to slightly deeper-water conditions than Facies Association B and the onset of a transgressive systems tract.

Facies Association D

This facies association is dominated by thrombolitic microbialites. Modern examples of non-laminated cerebroid, or thrombolitic, structures in Shark Bay formed from the rapid cementation of coccoidal cyanobacteria in the subtidal zone (Jahnert & Collins, 2012; Playford *et al.*, 2013). Using this modern analogue, it is suggested that the thrombolitic microbialites described here probably also

formed due to the activity of coccoidal bacteria, rather than filamentous, in a similar, deeper-water setting than either Facies Associations B or C. To accumulate 40 m of very homogenous thrombolitic microbialite, basin subsidence must have been at a rate which favoured the growth and rapid cementation of the clotted fabric and, perhaps, was too deep for large columnar stromatolites to flourish. It would appear from the consistent clotted fabric and only very localised development of thinly bedded sedimentary units (up to 10 cm thick), that basin deepening kept pace with the accumulation of the thrombolite-like microbial precipitation throughout the accumulation of this facies association. This rate of subsidence continued until a time when there was a transition into the deposition of bedded dolarenite represented by Facies Association E, either in an even deeper-water environment, possibly below the photic zone, or an environment of greater sediment supply.

Facies Association E

The turbidite sequence near the base of Facies Association E is suggestive of a basin slope environment, which is supported by an absence of storm deposits or other evidence of current reworking. The lack of conglomerates or breccias indicates deposition below storm wave base. Successive units of thinly bedded dololutite to dolarenite suggest basin deepening and deposition further away from the sediment source. The subsequent unit of very finely laminated ironstone is thought to represent the precipitates from a chemocline and supports deposition during progressive deepening. Following this, the transition up-section to shale represents a shift to a low-energy, even deeper-water setting, away from the influence and transport of distal carbonate sediment. Up-section from the shale is another unit of ironstone and black chert, followed by a return to dololutites. The symmetrically flanking units of dololutite, ironstone and black chert either side of the shale indicate it is the deepest part of the basin. At this point in the stratigraphy, it is proposed that the basin experienced a tectonic inflection point and/or a change from a transgressive to a regressive systems tract centred in the shale unit.

Summary

Analysis of water-depth indicators throughout the reef complex reveals it was deposited during parts of two regression sequences and one full transgression sequence (Fig. 20). The first regression extends from underlying siliciclastic units, through Facies Association A, to halfway through Facies Association B, ending with a period of very shallow water to possibly exposed conditions as represented by the horizontally branching stromatolites, pebble conglomerate unit and tepee structure. This was followed by a basin deepening, or transgression event, originating halfway through Facies Association B, and ending with the shale in the middle of Facies Association E. The upper regression sequence is marked by a return from the shale, through ironstone and black chert, to bedded dololutite. Neither the bottom nor top contacts of the reef complex as a whole are exposed.

Stratigraphic affinity

Several features of the Kazput stromatolite–thrombolite reef complex studied here have direct bearing on the issue of whether or not it could represent a structural slice of the younger Duck Creek Dolomite. First, detailed mapping shows that the studied reef complex is underlain by a thick succession of clastic sedimentary rocks that include a distinctive unit of rippled, quartz-rich sandstone (Figs 2 and 3A). Such a unit is not described for rocks of the Mt McGrath Formation that underlies the DCD (Seymour *et al.*, 1988), but correlates well with the Koolbye Formation of the Turee Creek Group in the type area of the Hardy Syncline (Mazumder *et al.*, 2015), supporting the placement of the studied reef complex within the Turee Creek Group, as first indicated by Trendall & Blockley (1970).

Second, map data and structural analysis show that the DCD is continuous along strike and affected only by a single generation of D_4 structures that include NW-trending, large-scale folds and dextral strike-slip faults (Fig. 1). In contrast, the reef complex here is associated with underlying rocks of the Turee Creek Group that are preserved in a series of faulted slices that strike E-W and have been affected by two main sets of structures, including E-W trending D_1 folds and the D_{2-3} structures noted above; this indicates that the studied ridge must belong to the older Turee Creek Group. Most significantly in this regard, D_{2-3} strike-slip faulting cannot account for the position of the reef complex studied here, were it to belong to the DCD, as the faults would have had to carve off an isolated sliver of the unit and uniquely juxtapose it down through 4 km of stratigraphy: such vertical fault movement has not been documented anywhere else in the southern Hamersley region and is inconsistent with the structural pattern of the DCD or adjacent units.

Third, the Kazput reef complex studied here shows very consistent $\delta^{13}C$ and $\delta^{18}O$ values (Fig. 19), in sharp contrast to the DCD that shows several significant excursions of both of these stable isotopes (Wilson *et al.*, 2010). Notably, the range of oxygen isotope values differs dramatically between the two units, with the main range of $\delta^{18}O$ values for the DCD varying between +2 and −8‰ (VPDB: Wilson *et al.*, 2010), whereas the Kazput Ridge reef complex has values that range from −10 to −15‰ (VPDB).

Fourth and most importantly are distinct stratigraphic and morphological differences between the two units. For example, the DCD is much thicker (1000 m thick) compared with the Kazput reef complex studied here (350 m thick). Also, the lower part of the DCD has numerous, repeated peritidal depositional cycles that give the formation a characteristic zebra-like appearance at this level: this feature is entirely lacking from the Kazput reef complex, where lower parts are characterised by thinly bedded, deeper-water dololutites. In addition, the DCD is characterised by the widespread development of microbialites with wrinkly laminations: this texture is entirely absent from the Kazput reef complex studied here. Finally, the Kazput reef complex contains two distinctive microbialite morphologies that are not documented for the DCD, including the thick section of clotty-textured, thrombolitic microbialite and the distinctive horizontally branching stromatolites.

In combination, these features show that the Kazput reef complex studied here is distinctly different from the younger DCD and does, in fact, represent a unit deposited as part of the Kazput Formation of the Turee Creek Group, immediately after the rise of atmospheric oxygen.

Secular evolution of microbialite morphology and fabric

In order to better understand the significance of microbialite features in the Kazput Formation stromatolite–thrombolite reef complex, we present a comparison with well-documented examples of both older (Neoarchean) and younger (Paleoproterozoic) examples of stromatolitic carbonate reefs (Table 2). Detailed studies on older, pre-GOE, stromatolitic carbonate reefs include the *c.* 2.6–2.5 Ga Campbellrand Subgroup in South Africa (Beukes, 1987; Sumner & Bowring, 1996; Sumner & Grotzinger, 2004; Sumner & Beukes, 2006; Schröder *et al.*, 2009) and the *c.* 2.6 Ga Carawine Dolomite of Western Australia (Simonson *et al.*, 1993), whilst the *c.* 1.8 Ga Duck Creek Dolomite represents a carbonate reef deposited post-GOE (Knoll & Barghoorn, 1976; Grey & Thorne, 1985; Knoll *et al.*, 1988; Veizer *et al.*, 1992; Lindsay & Brasier, 2002; Wilson *et al.*, 2010). The only broadly synchronous carbonate unit to the Kazput reef complex is the Espanola Formation (*c.* 2.5–2.15 Ga) of the Huronian Supergroup in Canada. However, this unit is only ~100 m thick and evidence for stromatolites is scarce, with only small columnar stromatolites, described to be on average 1 cm high (Hofmann *et al.*, 1980).

Campbellrand Subgroup

The well-documented *c.* 2.6–2.5 Ga Campbellrand Subgroup is a low metamorphic grade carbonate sequence in South Africa, ranging between 1500 and 1700 m thick (Beukes, 1987; Sumner & Bowring, 1996; Sumner & Grotzinger, 2004; Sumner & Beukes, 2006; Schröder *et al.*, 2009). A large, north-west trending growth fault divides the Campbellrand Subgroup into two main domains: the north-east, characterised by oolitic and stromatolitic carbonate platforms, and south-west, which con-

Table 2 Summary of key attributes of reef complexes from; Campbellrand Subgroup, Carawine Dolomite, Kazput Formation and Duck Creek Dolomite

	Campbellrand Subgroup	Carawine Dolomite	Kazput Formation	Duck Creek Dolomite
Age	*c.* 2.6–2.5 Ga	*c.* 2.6 Ga	*c.* 2.45–2.2 Ga	*c.* 1.8 Ga
Continuity of sequence	550 km long by 1500–1700 m thick	150–200 m thick sections of outcrop	15 km long by 350 m thick	1000 m thick sections of outcrop
Structural geology	Large growth fault splitting entire area into two domains. Some localised tight folds in carbonate	Undergone relatively little deformation, with low angle dips	One or two places for minor potential faulting, but little effect on litho-stratigraphic analysis	One possible area of localised faulting – little impact on litho-stratigraphic analysis
Characteristic lithologies, sedimentary features	Carbonate, shale, oolitic limestone, iron-formation, black chert, tuff	Dolomite with minor argillite and chert. Wave ripples and palisade textures	Dololutite, dolarenite, pebble conglomerate, shale, ironstone, black chert. Turbidites and tepee and dewatering structures	Carbonate, flat pebble conglomerate, ironstone, black chert, tuff. Turbidites and tepee structure
Key microbial morphologies	Giant stromatolite mounds and columnar, stratiform and dome-shaped stromatolites	LLH and SH-type stromatolites (Logan *et al.*, 1964), large stromatolitic mounds, large dome-shaped stromatolites and flat pebbles with oncolitic coatings	Columnar, stratiform, club-shaped, dome-shaped and horizontally branching stromatolites, and clotted thrombolite-like microbialite	Wrinkly microbial laminations and dome, conical, broad branching columnar, narrow tall columnar and club-shaped stromatolites
Transgression/ regression cycles	One widespread major transgression event	Insufficient data to quantify	Part regression at base, then whole transgression followed by another part regression	Open regression, transitioning to transgression. Maximum flood point reached, followed by regression and subsequent transgression event

tains interbedded microbialites, cherts and iron formation (Schröder *et al.*, 2009).

The main part of the carbonate platform in the north-east contains a non-stromatolitic sequence at the base (approximately 600 m thick) and an approximately 1500 m thick, overlying shallow-water stromatolitic carbonate sequence. This overlying sequence consists of giant stromatolite mounds and columnar, stratiform and dome-shaped stromatolites (Beukes, 1987; Sumner & Grotzinger, 2004). The large stromatolite mounds are elongated, closely spaced and laterally linked, and range in size from 1 to 10 m across, and up to 40 m in length. The dome-shaped stromatolites range from 50 to 100 cm wide and have a synoptic relief of up to 40 cm (Beukes, 1987).

Carawine Dolomite

The *c.* 2.6 Ga Carawine Dolomite is interpreted as a shallow-water carbonate platform that consists of dolomite, with minor interbeds of argillite and some chert nodules (Simonson *et al.*, 1993). The Carawine Dolomite contains abundant wave ripples, stromatolites and oncolites; the laterally linked hemispheroid-type (or LLH-type) stromatolites, as described by Logan *et al.* (1964), form one of the main constituent stromatolites. Other forms described are SH-type (stacked hemispheroids; Logan *et al.*, 1964) stromatolites, large stromatolitic mounds and large dome structures. The SH-type stromatolites are relatively small, ranging from only 1 to 6 cm wide and 20 cm high, whilst the stromatolite mounds can reach as large as 4.4 m wide and 1.2 m high. The stromatolite domes are relatively large, averaging 4.4 m high by 4 m wide, and reaching up to 15 m high. Other structures described include columnar stromatolites and palisade textures. Many of the stromatolites contain wavy irregular laminations. Simonson *et al.* (1993) make comparisons between the Carawine Dolomite and the Campbellrand Subgroup, indicating they contain similar fabrics and textures and were deposited at a similar time and in a similar environment.

Duck Creek Dolomite

The *c.* 1.8 Ga Duck Creek Dolomite (DCD) is a low metamorphic grade stromatolitic carbonate platform that crops out for 100's of kilometres and is approximately 1000 m thick (Grey & Thorne, 1985; Veizer *et al.*, 1992; Lindsay & Brasier, 2002; Wilson *et al.*, 2010). At its type section in Duck Creek, the DCD consists of a series of multiple transgression–regression cycles, containing stromatolitic parasequences, minor iron formation and microfossil-hosting black chert units.

Wilson *et al.* (2010) divide the DCD into three sequences. Sequence 1 at the base of the formation contains part of a regressive cycle and consists of dolostone with tepee structures, flat-pebble conglomerates and symmetrical wave-action ripples. It is interpreted as a high energy, shallow-water environment and is the only part of the DCD which displays sedimentary features other than stromatolites (Wilson *et al.*, 2010). Sequence 2 comprises a transgressive series containing columnar stromatolites capped by a ~1-m-thick unit of iron formation, as well as a regressive series, characterised by peritidal parasequences, containing stromatolites with low synoptic relief. Sequence 3 represents another transgressive phase and consists of interbedded dolomite grainstones, which grade up into columnar stromatolites. These units are capped by a thicker section of iron formation and shale, designating the maximum flooding interval (Wilson *et al.*, 2010).

Stromatolite morphology in the Duck Creek Dolomite is diverse, with thick sections of stratiform microbialite characterised by wrinkly laminations, low broad domical forms, units with tightly packed coniform stromatolites, broad branching columnar stromatolites with synoptic relief of up to 10 cm, narrow tall, branching columnar stromatolites and club-shaped stromatolites (e.g. Walter, 1972; Grey, 1985; Grey & Thorne, 1985; Van Kranendonk, 2010).

Changes in microbialite morphology over time

Neoarchean and all other older stromatolites (e.g. Hofmann *et al.*, 1999) are distinctly simpler, in terms of their branching morphology, than Paleoproterozoic stromatolites and in particular, those of the Kazput reef complex described here. The most significant differences between the Kazput reef complex and the Neoarchean carbonate reefs summarised here are the clotty-textured thrombolitic microbialite and stromatolites with complex branching patterns, including horizontal branching. Indeed, given the *c.* 2.4–2.3 Ga age of the Kazput reef complex at the very onset of the Proterozoic Eon, these two distinctive features represent the oldest occurrences in the geological record.

Similar to thrombolites in the *c.* 1.9 Ga Rocknest Formation (Kah & Grotzinger, 1992), the clotted microbialite of the Kazput reef complex is also similar to modern thrombolitic structures in Shark Bay, which form from the rapid cementation of coccoidal cyanobacteria (Kennard & James, 1986; Grotzinger, 1990; Jahnert & Collins, 2012). Although coccoid cyanobacterial remnants have been described from the Neoarchean Campbellrand Subgroup (Kazmierczak *et al.*, 2009), thrombolitic microbialites have not. Thus, we posit the Kazput clotted microbialites could have arisen immediately following the GOE.

Younger Paleoproterozoic microbialite reef complexes contain some similarities to the Kazput reef complex, including complex branching stromatolite forms and even thrombolites (e.g. Kah & Grotzinger, 1992; Kah *et al.*, 2009). However, one difference between these units is that the younger deposits (as, for example, the *c.* 1.8 Ga DCD) preserve widespread, wrinkly lamination that is absent from the Kazput reef complex. The reason for this distinctive

morphology in *c.* 1.8 Ga microbialites is not known. Although it may simply relate to the degree of preservation, it could also reflect different environments of deposition and/or a more complex growth pattern in the younger units.

The fact that the Kazput reef complex was deposited directly after the rise of atmospheric oxygen invites consideration as to whether this rise in some way caused the textural changes observed in the microbialites. However, the role of environment vs evolution in stromatolite morphological studies has always been controversial (Walter, 1972). We do not yet have enough information from this, and other reef complexes, to know whether the rise of atmospheric oxygen had anything to do with the morphological changes described here. Certainly, however, the fact that complex branching appears to dominate in post-2.5 Ga carbonate reefs vs pre-2.5 Ga reefs suggests that something quite fundamental occurred across the Archean–Proterozoic boundary, but what this was remains to be determined.

CONCLUSION

The Kazput reef complex of the Turee Creek Group is an extremely well preserved 350 m thick by 15 km long unit of stromatolitic-thrombolitic dolostone, with subordinate shale, thinly bedded ironstone and black chert. Stratigraphically, structurally and isotopically distinct from the nearby, *c.* 1.8 Ga Duck Creek Dolomite, the Kazput reef complex represents the oldest occurrence of an extensive marine carbonate reef complex immediately following the rise of atmospheric oxygen, providing a window on the adaptation of life at this time.

The reef complex displays clear primary textural features and distinctive sedimentary and organosedimentary fabrics. Five stacked facies associations that are continuous along the length of exposure are interpreted to reflect a part marine regression at the base, a transgression through the middle, and part of another marine regression at the top.

The Kazput reef complex contains a globally unique occurrence of 1.5-m-high columnar stromatolites with sets of horizontally extending branches. The reef complex also contains the oldest known occurrence of thick, clotted microbialite, interpreted to be thrombolite-like on the basis of comparison with the *c.* 1.9 Ga Rocknest Formation (Kah & Grotzinger, 1992) and modern microbialites in Shark Bay, Western Australia. Such complex branching stromatolite forms and extensive clotted microbialite denote the first appearances of more complex morphological growth in the geological record.

ACKNOWLEDGMENTS

We thank M.R. Walter, P. Phillipot, L.C. Kah and two anonymous reviewers for their helpful suggestions, which have greatly improved this manuscript. We also thank J. Jesse for field assistance. EB and MVK were supported by the Australian Research Council Centre of Excellence for Core to Crust Fluid Systems (http://ccfs.mq.edu.au/), and this is publication number 697 of that centre.

REFERENCES

Aitken JD (1967) Classification and environmental significance of cryptalgal limestones and dolomites, with illustrations from the Cambrian and Ordovician of southwestern Alberta. *Journal of Sedimentary Research* **37**, 1163–1178.

Barley ME, Pickard AL, Sylvester PJ (1997) Emplacement of a large igneous province as a possible cause of banded iron formation 2.45 billion years ago. *Nature* **385**, 55–58.

Barlow E (2014) Stratigraphy and petrography of a Paleoproterozoic carbonate reef from the Turee Creek Group, Western Australia. Unpublished Honours thesis: University of New South Wales, Sydney, Australia, 78 p.

Bartley JK, Kah LC, Frank TD, Lyons TW (2014) Deep-water microbialites of the Mesoproterozoic Dismal Lakes Group: microbial growth, lithification, and implications for coniform stromatolites. *Geobiology* **13**, 15–32.

Beukes NJ (1987) Facies relations, depositional environments and diagenesis in a major early Proterozoic stromatolitic carbonate platform to basinal sequence, Campbellrand Subgroup, Transvaal Supergroup, Southern Africa. *Sedimentary Geology* **54**, 1–46.

Blight DF, Seymour DB, Thorne AM (1986) Wyloo, Western Australia (Second Edition): 1:250 000 Geological Map (Sheet SF 50-10). *Geological Survey of Western Australia*.

Castiglioni C, Mapelli C, Negri F, Zerbi G (2001) Origin of the D line in the Raman spectrum of graphite: a study based on Raman frequencies and intensities of polycyclic aromatic hydrocarbon molecules. *The Journal of Chemical Physics* **114**, 963–974.

Donaldson JA (1976) Chapter 10.2 Paleoecology of Conophyton and Associated Stromatolites in the Precambrian Dismal Lakes and Rae Groups, Canada. In: *Stromatolites. Developments in Sedimentology, No. 20* (ed. Walter MR). Elsevier, Amsterdam, pp. 523–534.

Evans DAD, Sircombe K, Wingate MTD, Doyle M, McCarthy M, Pidgeon RT, Van Niekerk HS (2003) Revised geochronology of magmatism in the western Capricorn Orogen at 1805-1785 Ma: diachroneity of the Pilbara-Yilgarn collision. *Australian Journal of Earth Sciences* **50**, 853–864.

Farquhar J, Wing BA (2003) Multiple sulfur isotopes and the evolution of the atmosphere. *Earth and Planetary Science Letters* **213**, 1–13.

Farquhar J, Bao H, Thiemens M (2000) Atmospheric Influence of Earth's Earliest Sulfur Cycle. *Science* **289**, 756–758.

Gandin A, Wright DT, Melezhik V (2005) Vanished evaporites and carbonate formation in the Neoarchaean Kogelbeen and Gamohaan formations of the Campbellrand Subgroup, South Africa. *Journal of African Earth Sciences* **41**, 1–23.

Gebelein CD (1976) Chapter 8.1 Open Marine Subtidal and Intertidal Stromatolites (Florida, The Bahamas and Bermuda). In: *Stromatolites. Developments in Sedimentology, No. 20* (ed. Walter MR). Elsevier, Amsterdam, pp. 381–388.

Goldblatt C, Lenton TM, Watson AJ (2006) Bistability of atmospheric oxygen and the Great Oxidation. *Nature* **443**, 683–686.

Grey K (1985) Stromatolites in the Duck Creek Dolomite, Western Australia. Geological Survey of Western Australia, Report 14, Professional Papers for 1983, pp. 94–103.

Grey K, Thorne AM (1985) Biostratigraphic significance of stromatolites in upward shallowing sequences of the Early Proterozoic Duck Creek Dolomite, Western Australia. *Precambrian Research* **29**, 183–206.
Grotzinger JP (1990) Geochemical model for Proterozoic stromatolite decline. *American Journal of Science*, **290-A**, 80–103.
Hannah JL, Bekker A, Stein HJ, Markey RJ, Holland HD (2004) Primitive Os and 2316 Ma age for marine shale: implications for Paleoproterozoic glacial events and the rise of atmospheric oxygen. *Earth and Planetary Science Letters* **225**, 43–52.
Hoffman P (1976) Chapter 6.1 Stromatolite Morphogenesis in Shark Bay, Western Australia. In: *Stromatolites. Developments in Sedimentology, No. 20* (ed. Walter MR). Elsevier, Amsterdam, pp. 261–271.
Hofmann HJ, Jackson GD (1987) Proterozoic ministromatolites with radial-fibrous fabric. *Sedimentology* **34**, 963–971.
Hofmann HJ, Pearson DAB, Wilson BH (1980) Stromatolites and fenestral fabric in Early Proterozoic Huronian Supergroup, Ontario. *Canadian Journal of Earth Sciences* **17**, 1351–1357.
Hofmann HJ, Grey K, Hickman AH, Thorpe R (1999) Origin of 3.45 Ga coniform stromatolites in the Warrawoona Group, Western Australia. *Geological Society of America Bulletin* **111**, 1256–1262.
Holland HD (1994) Early Proterozoic atmosphere change. In *Early life on earth.* (ed. Bengtson S). Columbia University Press, New York, pp. 237–244.
Holland HD (2002) Volcanic gases, black smokers, and the Great Oxidation Event. *Geochimica et Cosmochimica Acta* **66**, 3811–3826.
Holland HD (2006) The oxygenation of the atmosphere and oceans. *Philosophical Transactions of the Royal Society B* **361**, 903–915.
Jahnert RJ, Collins LB (2012) Characteristics, distribution and morphogenesis of subtidal microbial systems in Shark Bay, Australia. *Marine Geology* **303–306**, 115–136.
Kah LC, Grotzinger JP (1992) Early Proterozoic (1.9 Ga) Thrombolites of the Rocknest Formation, Northwest Territories, Canada. *Palaios* **7**, 305–315.
Kah LC, Bartley JK, Stagner AF (2009) Reinterpreting a Proterozoic Enigma: Conophyton-Jacutophyton Stromatolites of the Mesoproterozoic Atar Group, Mauritania. *International Association of Sedimentologists Special Publication* **41**, 277–295.
Kazmierczak J, Altermann W, Kremer B, Kempe S, Eriksson PG (2009) Mass occurrence of benthic coccoid cyanobacteria and their role in the production of Neoarchean carbonates of South Africa. *Precambrian Research* **173**, 79–92.
Kennard JM, James NP (1986) Thrombolites and Stromatolites: two distinct types of microbial structures. *Palaios* **1**, 492–503.
Knoll AH, Barghoorn E (1976) A Gunflint-type microbiota from the Duck Creek dolomite, Western Australia. *Origins of Life* **7**, 417–423.
Knoll AH, Strother PK, Rossi S (1988) Distribution and diagenesis of microfossils from the lower Proterozoic Duck Creek Dolomite, Western Australia. *Precambrian Research* **38**, 257–279.
Kudryavtsev AB, Schopf JW, Agresti DG, Wdowia TJ (2000) *In situ* laser-Raman imagery of Precambrian microscopic fossils. *Proceedings of the National Academy of Sciences of the United States of America* **98**, 823–826.
Lindsay JF, Brasier MD (2002) Did global tectonics drive early biosphere evolution? Carbon isotope record from 2.6 to 1.9 Ga carbonates of Western Australian basins. *Precambrian Research* **114**, 1–34.
Logan BW, Rezak R, Ginsburg RN (1964) Classification and Environmental Significance of Algal Stromatolites. *The Journal of Geology* **72**, 68–83.
Margulis L, Sagan D (1997) *Microcosmos: Four Billion Years of Evolution from Our Microbial Ancestors.* University of California Press, Berkeley. 304 pp.
Marshall CP, Emry JR, Marshall AO (2011) Haematite pseudomicrofossils present in the 3.5-billion-year-old Apex Chert. *Nature Geoscience* **4**, 240–243.
Martin DM (1999) Depositional setting and implications of Paleoproterozoic glaciomarine sedimentation in the Hamersley Province, Western Australia. *Geological Society of America Bulletin* **111**, 189–203.
Martin DM, Morris PA (2010) Tectonic setting and regional implications of ca 2.2 Ga mafic magmatism in the southern Hamersley Province, Western Australia. *Australian Journal of Earth Sciences* **57**, 911–931.
Martin DM, Li ZX, Nemchin AA, Powell CM (1998) A pre-2.2 Ga age for giant hematite ores of the Hamersley Province, Australia? *Economic Geology* **93**, 1084–1090.
Martin DM, Powell CM, George AD (2000) Stratigraphic architecture and evolution of the early Paleoproterozoic McGrath Trough, Western Australia. *Precambrian Research* **99**, 33–64.
Martindale R, Strauss JV, Sperling EA, Johnson JE, Van Kranendonk MJ, Flannery DT, French K, Lepot K, Mazumder R, Rice MS, Schrag DP, Summons R, Walter M, Abelson J, Knoll AH (2015) Sedimentology, chemostratigraphy, and stromatolites of lower Paleoproterozoic carbonates, Turee Creek Group, Western Australia. *Precambrian Research* **266**, 194–211.
Mazumder R, Van Kranendonk MJ (2013) Palaeoproterozoic terrestrial sedimentation in the Beasley River Quartzite, lower Wyloo Group, Western Australia. *Precambrian Research* **231**, 98–105.
Mazumder R, Van Kranendonk MJ, Altermann W (2015) A marine to fluvial transition in the Paleoproterozoic Koolbye Formation, Turee Creek Group, Western Australia. *Precambrian Research* **258**, 161–170.
Müller SG, Krapež B, Barley ME, Fletcher IR (2005) Giant iron-ore deposits of the Hamersley province related to the breakup of Paleoproterozoic Australia: new insights from *in situ* SHRIMP dating of baddeleyite from mafic intrusions. *Geology* **33**, 577–580.
Papineau D (2010) Global biogeochemical changes at both ends of the Proterozoic: insights from phosphorites. *Astrobiology* **10**, 165–181.
Playford PE, Cockbain AE (1976) Chapter 8.2 Modern Algal Stromatolites at Hamelin Pool, A Hypersaline Barred Basin in Shark Bay, Western Australia. In: *Stromatolites. Developments in Sedimentology, No. 20* (ed. Walter MR). Elsevier, Amsterdam, pp. 389–411.
Playford PE, Cockbain AE, Berry PF, Roberts AP, Haines PW, Brooke BP (2013) The geology of Shark Bay. *Geological Survey of Western Australia Bulletin* **146**, 281.
Rasmussen B, Fletcher IR, Sheppard S (2005) Isotopic dating of the migration of a low-grade metamorphic front during orogenesis. *Geology* **33**, 773–776.
Riding R (1999) The term stromatolite: towards an essential definition. *Lethaia* **32**, 321–330.
Schopf JW, Kudryavtsev AB, Agresti DG, Wdowiak TJ, Czaja AD (2002) Laser-Raman imagery of Earth's earliest fossils. *Nature* **416**, 73–76.
Schopf JW, Kudryavtsev AB, Agresti DG, Czaja AD, Wdowiak TJ (2005) Raman imagery: a new approach to assess the

geochemical maturity and biogenicity of permineralized Precambrian fossils. *Astrobiology* **5**, 333–371.
Schröder S, Beukes NJ, Sumner DY (2009) Microbialite–sediment interactions on the slope of the Campbellrand carbonate platform (Neoarchean, South Africa). *Precambrian Research* **169**, 68–79.
Seymour DB, Thorne AM, Blight DF (1988) Wyloo, Western Australia (Second Edition): 1:250 000 Geological Series. *Geological Survey of Western Australia, 1:250 000 Geological Series – Explanatory Notes.*
Simonson BM, Schubel KA, Hassler SW (1993) Carbonate sedimentology of the early Precambrian Hamersley Group of Western Australia. *Precambrian Research* **60**, 287–335.
Smith RE, Perdrix JL, Parks TC (1982) Burial Metamorphism in the Hamersley Basin, Western Australia. *Journal of Petrology* **23**, 75–102.
Summons RE, Hallmann C (2014) Organic Geochemical Signatures of Early Life on Earth. In *Treatise on Geochemistry*, 2nd edn. (eds Holland HD, Turekian KK). Elsevier, Oxford, pp. 33–46.
Sumner DY, Beukes NJ (2006) Sequence Stratigraphic Development of the Neoarchean Transvaal carbonate platform, Kaapvaal Craton, South Africa. *South African Journal of Geology* **109**, 11–22.
Sumner DY, Bowring SA (1996) U-Pb geochronologic constraints on deposition of the Campbellrand Subgroup, Transvaal Supergroup, South Africa. *Precambrian Research* **79**, 25–35.
Sumner DY, Grotzinger JP (1996) Herringbone calcite: petrography and environmental significance. *Journal of Sedimentary Research* **66**, 419–429.
Sumner DY, Grotzinger JP (2004) Implications for Neoarchaean ocean chemistry from primary carbonate mineralogy of the Campbellrand-Malmani Platform, South Africa. *Sedimentology* **51**, 1273–1299.
Swanner ED, Bekker A, Pecoits E, Konhauser KO, Cates NL, Mojzsis SJ (2013) Geochemistry of pyrite from diamictites of the Boolgeeda Iron Formation, Western Australia with implications for the GOE and Paleoproterozoic ice ages. *Chemical Geology* **362**, 131–142.
Takehara M, Komure M, Kiyokawa S, Horie K, Yokohama K (2010) Detrital zircon SHRIMP U-Pb age of the 2.3 Ga diamictites of the Meteorite Bore Member in the South Pilbara, Western Australia. In *Fifth International Archean Symposium Abstracts* (eds Tyler IM, Knox-Robinson CM). Geological Survey of Western Australia, Record 2010/18, 223–224.
Thorne AM, Tyler IM (1996) Geology of the Rocklea 1:100 000 sheet. *Geological Survey of Western Australia, 1:100 000 Series – Explanatory Notes.*
Trendall AF (1981) The Lower Proterozoic Meteorite Bore Member, Hamersley Basin Western Australia. In *Earth's Pre-Pleistocene Glacial Record.* (eds Hambrey MJ, Harland WB). Cambridge University Press, Cambridge, pp. 555–557.
Trendall AF, Blockley JG (1970) The iron formations of the Precambrian Hamersley Group, Western Australia, with special reference to the associated crocidolite. *Geological Survey Western Australia Bulletin*, **119**, 366.
Trendall AF, Compston W, Nelson DR, De Laeter JR, Bennett VC (2004) SHRIMP zircon ages constraining the depositional chronology of the Hamersley Group, Western Australia. *Australian Journal of Earth Sciences* **51**, 621–644.
Tuinstra F, Koenig JL (1970) Raman Spectrum of Graphite. *The Journal of Chemical Physics* **53**, 1126–1130.
Tyler IM, Thorne AM (1990) The northern margin of the Capricorn Orogen, Western Australia – An example of an Early Proterozoic collision zone. *Journal of Structural Geology* **12**, 685–701.
Van Kranendonk MJ (2010) Three and a half billion years of life on Earth: a transect back into deep time. *Geological Survey of Western Australia*, Record 2010/21, 93 p.
Van Kranendonk MJ (2014) Earth's early atmosphere and surface environments: a review. *Geological Society of America Special Papers* **504**, 105–130.
Van Kranendonk MJ, Mazumder R (2015) Two Paleoproterozoic glacio-eustatic cycles in the Turee Creek Group, Western Australia. *Geological Society of America Bulletin* **127**, 596–607.
Van Kranendonk MJ, Mazumder R, Yamaguchi KE, Yamada K, Ikehara M (2015) Sedimentology of the Paleoproterozoic Kungarra Formation, Turee Creek Group, Western Australia: a conformable record of the transition from early to modern Earth. *Precambrian Research* **256**, 314–343.
Veizer J, Clayton RN, Hinton RW (1992) Geochemistry of Precambrian carbonates: IV. Early Paleoproterozoic (2.25 ± 0.25 Ga) seawater. *Geochimica et Cosmochimica Acta* **56**, 875–885.
Walter MR (1972) Stromatolites and the biostratigraphy of the Australian Precambrian and Cambrian. *Special Papers in Paleontology* **11**, 256.
Williford KH, Van Kranendonk MJ, Ushikubo T, Kozdon R, Valley JW (2011) Constraining atmospheric oxygen and seawater sulfate concentrations during Paleoproterozoic glaciation: *In situ* sulfur three-isotope microanalysis of pyrite from the Turee Creek Group, Western Australia. *Geochimica et Cosmochimica Acta* **75**, 5686–5705.
Wilson JP, Fischer WW, Johnston DT, Knoll AH, Grotzinger JP, Walter MR, McNaughton NJ, Simon M, Abelson J, Schrag DP, Summons R, Allwood A, Andres M, Gammon C, Garvin J, Rashby S, Schweizer M, Watters WA (2010) Geobiology of the late Paleoproterozoic Duck Creek Formation, Western Australia. *Precambrian Research* **179**, 135–149.

SUPPORTING INFORMATION

Additional Supporting Information may be found in the online version of this article:

Fig. S1. Columnar stromatolite – original spectra.

Fig. S2. Columnar stromatolite – baseline corrected using 4 points.

Fig. S3. Oncolite – original spectra.

Fig. S4. Oncolite – baseline corrected using 4 points.

Fig. S5. Oncolite – baseline corrected, peak pick.

Fig. S6. Clotted microbialite – original spectra.

Fig. S7. Clotted microbialite – baseline corrected using 4 points.

Fig. S8. Clotted microbialite – baseline corrected, peak pick.